Biopharmaceutical characterization: Improve predictive screening

How to achieve deeper characterization of biotherapeutic proteins using light scattering

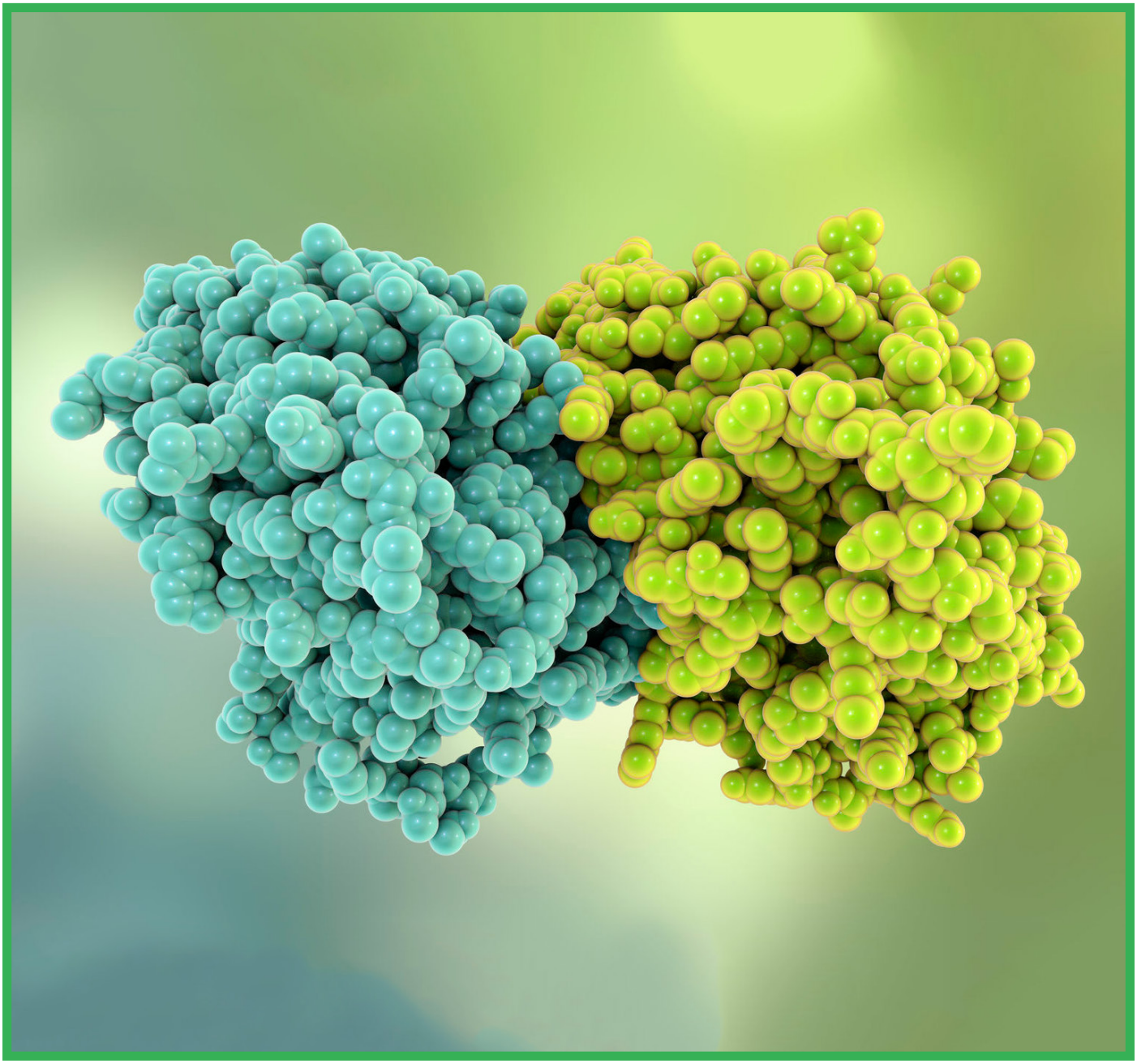

THE QUEEN'S AWARDS FOR ENTERPRISE: INTERNATIONAL TRADE 2021

BROUGHT TO YOU BY INDEPENDENT SCIENCE PUBLISHER

SelectScience®

IN PARTNERSHIP WITH

WYATT TECHNOLOGY

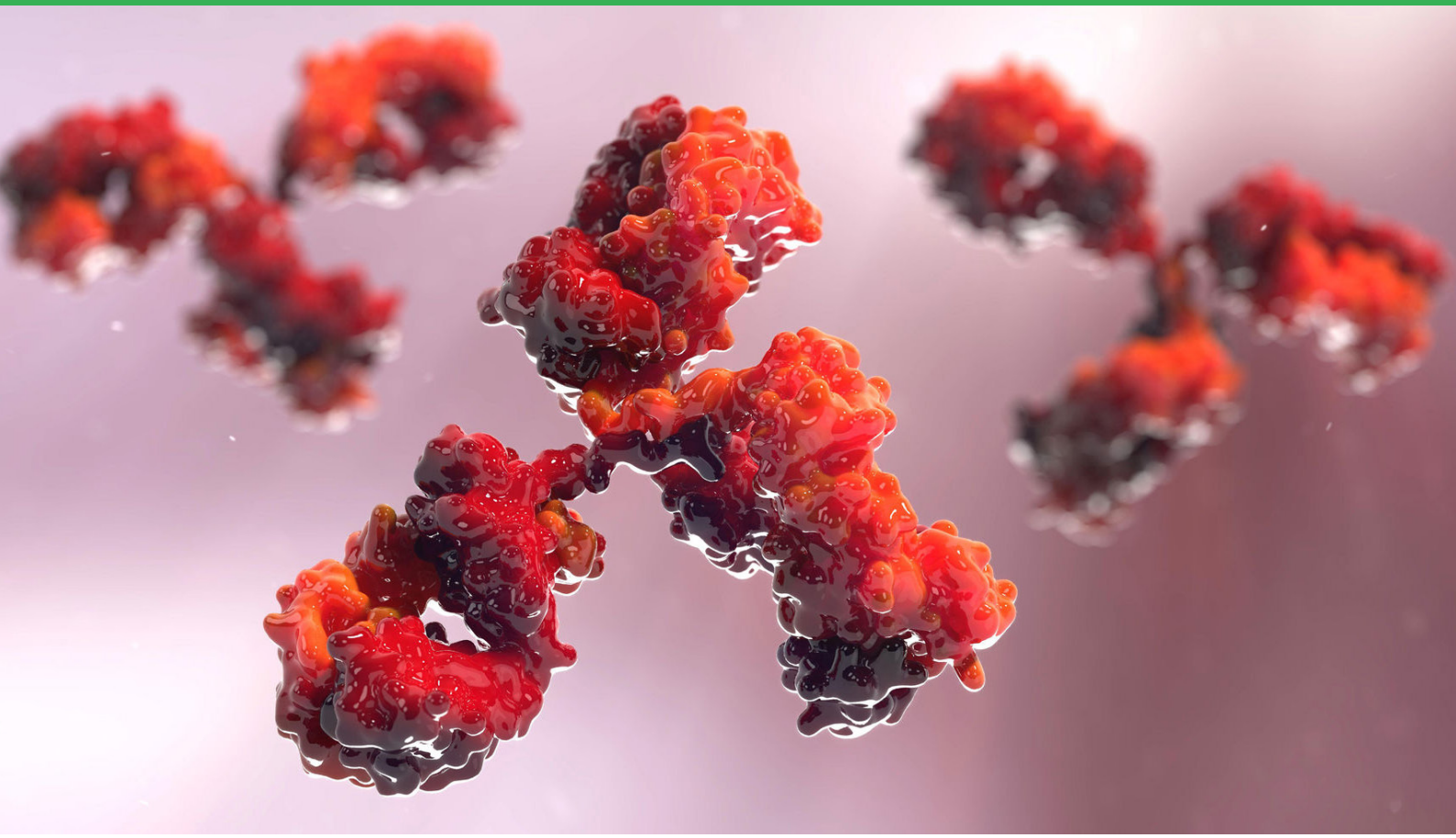

Introduction

Biopharmaceuticals, comprising monoclonal antibodies, antibody-drug conjugates, recombinant or fusion proteins, and bispecifics, among others, have recently gained commercial success and are rapidly changing the therapeutic landscape.

Due to their large size and complex structures, characterizing these biotherapeutics requires robust and demanding analytical techniques. Often, traditional methods used to characterize proteins fail to deliver on either the sensitivity required or the speed desired to accelerate the drug development pipeline.

Providing a versatile and reliable approach to biotherapeutic characterization, light scattering techniques are now becoming widely utilized to characterize macromolecules in solution. Contrary to most characterization methods, light scattering methods don't rely on external calibration standards – they provide absolute measurements.

Light scattering techniques can be employed at almost every stage of the drug development pipeline – target discovery, selection, optimization, purification, formulation, and manufacturing. For instance,

Contents

size-exclusion chromatography combined with multi-angle light scattering (SEC-MALS) can characterize biomolecules for aggregates, while composition-gradient, multi-angle light scattering (CG-MALS) is well suited to examine interactions. Meanwhile, high-throughput dynamic light scattering (DLS) can be used to access the different stability parameters of a drug formulation.

In this eBook, we've curated characterization approaches for different types of biotherapeutics, all using light scattering methods:

Identify insulin oligomeric states

A key step to ensure the safety, stability, and performance of insulin formulations is to examine and identify the oligomeric species present in the preparation. Here, SEC-MALS is applied to identify monomers, dimers, hexamers, and higher aggregates of insulin in three different sample preparations.

Compared to the traditional SEC method that separates the molecules based on their hydrodynamic volumes, not molar mass, MALS provides greater accuracy. It measures molar mass in an absolute manner using first principles, making it more reliable to investigate oligomerization.

Characterize monoclonal antibodies and antibody-drug conjugates (ADCs)

Prone to aggregation caused by the intermolecular interactions, ADC complexes need to be monitored for stability during formulation to ensure that the desired safety and commercial standards are maintained. In this application note, two ADCs based on monoclonal antibodies IgG1 and IgG2 are characterized using high-throughput DLS on the DynaPro® Plate Reader.

Additionally, formulation screening using automated, high-throughput DLS in multi-well plates boosts productivity and saves time compared to the traditional, labor-intensive batching methods.

Characterize self-associating antibody solutions

Self-interactions among protein molecules within a therapeutic formulation can severely impact solution viscosity and colloidal stability. MALS is uniquely suited to quantify these weak protein-protein interactions as it enables measurements in solution without tagging, immobilization, or other sample modifications.

In this study, the self-association affinity and stoichiometry of three antibody formulations in their corresponding formulation buffers were quantified using CG-MALS, employing the Calypso® biomolecular interaction analysis system for the concentration gradient and the DAWN® multi-angle light scattering (MALS) detector.

Quantify insulin self-association

The ability to modify the desired self-association state of insulin analogs directly influences the underlying pharmacokinetic and pharmacodynamic profiles. As such, the analogs may then be suitable for either fast-action or slow-release applications, making it integral to accurately quantify the affinity and stoichiometry of insulin self-association in pharmaceutical preparations. This application note demonstrates how CG-MALS was used to quantify the self-association of insulin at neutral pH in the absence of $Zn^{2}+$ in a label-free manner.

Measure colloidal and thermal stability

Stability is a key quality attribute that is tested during the formulation stage of a biotherapeutic. A variety of stability-indicating parameters, such as colloidal and thermal stability, are typically measured using rapid screens. In this experiment, high-throughput DLS was used to simultaneously determine thermal and colloidal stability, along with actual aggregation states, maximizing the information obtained from one run, thus boosting overall productivity.

Assess drug candidate suitability

To minimize the risk of failure during drug development, drug candidates are assessed for their suitability and developability during the earlier stages. Of the parameters measured, homogeneity, stability, and viscosity are significant factors that can influence the drug's performance, delivery methods, and manufacturing feasibility. This white paper outlines why DLS is a particularly effective method to assess drug candidates and inspect these key parameters in a high-throughput format.

Analyze protein aggregation
Learn how three orthogonal light scattering techniques complement each other to analyze and quantify soluble and sub-micron insoluble aggregates. This poster describes the capabilities of SEC-MALS, FFF-MALS and CG-MALS and how they work together to provide a comprehensive picture of irreversible and reversible aggregates.

Applying light scattering techniques at the different stages of biotherapeutic development, from target discovery to formulation analysis, carries substantial benefits that can accelerate the drug development pipeline. Namely, scientists can:

- Identify the best candidates as early as possible
- Reduce unnecessary time sinks by focusing efforts on the most suitable candidates
- Facilitate high-throughput operations to boost productivity
- Obtain accurate, reliable, and reproducible results to confidently advance to the next step

Detailed, reliable characterization and rapid predictive screening will ultimately result in safe and highly effective therapeutics reaching the market faster.

WYATT TECHNOLOGY

APPLICATION NOTE

AN1605: Identification of insulin oligomeric states using SEC-MALS

P. Wahlund, Ph.D.[1], D. Roessner, Ph.D.[2] and T. Jocks, Ph.D. [2] [1]Novo Nordisk A/S [2]Wyatt Technology Corp.

Summary

Insulin, one of the most important mammalian hormones, regulates a multitude of metabolic functions including the control of the blood glucose level in the body. Under healthy conditions, insulin is produced and stored in the islet tissues of the pancreas and released depending on the metabolic situation. In patients suffering from diabetes, insulin cannot be sufficiently produced by the body. It has to be administered as a pharmakon via oral or injection pathways.

Under physiological conditions, insulin forms hexamer complexes in the presence of zinc ions. In the pancreas the hormone is also stored as zinc complexes. In pharmacological preparations therefore zinc is added to enable complex formation. To ensure safe and effective administration of insulin formulations, it is of vital interest to investigate, which oligomeric species are present in a specific preparation.

This application note shows how the combination of column chromatography (SEC/GPC) with Multi-Angle Light Scattering (MALS), Dynamic Light Scattering (DLS) and RI detection can be applied as a powerful tool to identify monomers, dimers, hexamers and higher aggregates of insulin. Using this approach, each preparation can be comprehensively characterized to determine optimal formulation, storage and administration conditions tor the patient's benefit.

Introduction

In the analysis of proteins and peptides the question arises frequently whether the molecules under investigation are monomeric or form dimers or higher aggregates. The knowledge of this stoichiometric relation enables the investigator to estimate if the protein is present in its biologically active form.

In such determinations the first step is usually the separation of the molecular species and their characterization.

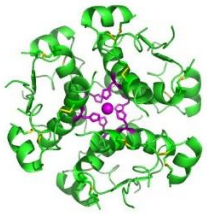

To achieve this, size exclusion chromatography (SEC) is often used as the method of choice. Since this approach separates the molecules according to their hydrodynamic volumes, it does not automatically allow the exact mass determination because molar mass is not necessarily a function of retention time but rather due to hydrodynamic properties.

A technology which overcomes this limitation is multi- angle light scattering (MALS). MALS measures molar mass in an absolute manner. This means no assumptions on the molecule's structure are made and no molar mass standards are needed. The determination relies on first principle measurements only and is therefore absolute. The MALS detection can be coupled to online DLS measurement to obtain hydrodynamic radii of the molecules. Moreover, CG-MALS measurements have been shown to be useful to detect the aggregation status of insulin[1,2].

The subject of the investigations presented here is the hormone insulin. Insulin plays a vital role in the regulation of mammalian blood glucose level and metabolism, cell growth and fat metabolism – only to name a few of its manifold functions. The discovery of insulin in 1921 represented a starting point for a revolution in the treatment of diabetes. Human insulin is a protein consisting of two peptide chains of 21 and 30 amino acids respectively, with total molar mass of 5.8 kDa. Human insulin self-associates and in the presence of zinc ions a hexameric complex is formed, 2 zinc ions bind per hexamer. Insulin is

stored in the β–cells of the pancreas as zinc complexes. In pharmaceutical preparations insulin is normally formulated at concentrations where the self-association is pronounced and hence zinc is added to stabilize the hexamer and thereby a more stable formulation. Upon dilution after delivery the hexamer dissociates and ends up as monomers in the blood stream. Hence it is of interest to investigate the oligomerization both from a formulation as well as pharmacological perspective.

Materials and Methods

An Agilent 1260 HPLC system was used which included an auto sampler, an isocratic pump and a degasser. The separation column was a Superose 12 300/10 from GE Healthcare.

For the detection we used a variable wavelength detector at 280 nm (Agilent), a DAWN® 18-angle light scattering detector equipped with a WyattQELS™ for online DLS detection, and an Optilab® refractive index detector. Molar masses were calculated from the MALS and dRI signals. The MALS, DLS and dRI detection instruments, as well as ASTRA® software for SEC-MALS analysis, were from Wyatt Technology.

The mobile phase consisted of 10 mM Tris, 140 mM NaCl, 2 mM Phenol and 200 ppm NaN3 at pH = 7.7.

Three different insulin sample preparations all containing 0.6 mM insulin were analyzed:

- Sample 1: insulin analogue without added zinc
- Sample 2: human insulin with 0.1 mM zinc
- Sample 3: human insulin with 0.3 mM zinc

Results and Discussion

Reversible protein assembly that increases with protein concentration, or self-association, is a well-known effect for e.g. monoclonal antibodies and insulin[3]. In the case of insulin, the molecule forms dimers and other oligomers which can be separated by SEC and detected by light scattering techniques[4,5]. Here we show the characterization of different insulin preparations by SEC-MALS.

Oligomers and self-association

Results of Sample 1 are shown with molar masses indicated throughout the chromatogram (Figure 1). The major fraction with molar mass corresponding to a monomer is well separated from the very minor fraction corresponding to hexamer, and the molar mass is observed to be quite uniform across the main peak. Although not present as resolved peaks in UV, MALS analysis indicates a molar mass distribution that covers the range from monomer to hexamer.

It should be emphasized that light scattering identified the hexamer easily even though the UV signal suggests that only a very small amount of this fraction is present. This is due to the extremely high sensitivity of the LS detection method for large molecules.

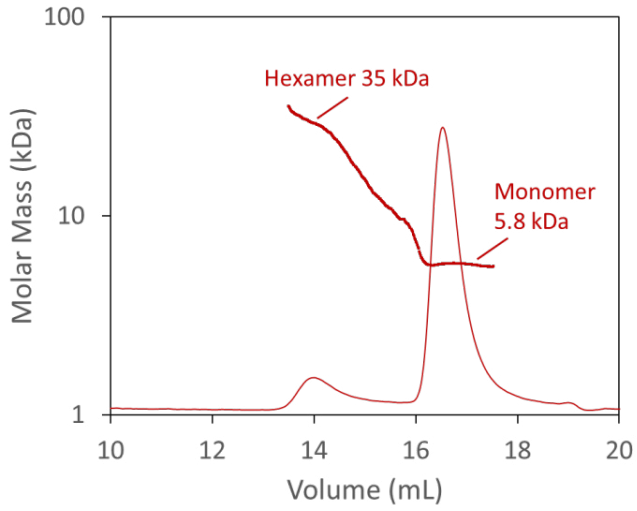

Figure 1. Plot of molar mass vs. time of Sample 1. The UV signal @ 280 nm is plotted as an overlay.

Formulation effects

Comparing sample 1 and 2 shows that the addition of 0.1 mM zinc lead to a shift in the equilibrium, going from mainly monomer in sample 1 to major fraction hexamer in Sample 2 (Figure 2). It is apparent from MALS analysis (not obvious from UV) that monomers and dimers exists in the minor peak of sample 2 and that the major peak is the hexamer.

Despite the long tail of the hexamer peak, MALS rules out the presence of oligomers with molar masses between dimer and hexamer. The tail is a result of non-ideal interactions between the hexamers and the column packing.

The presence of monomers and dimers, with the fraction of dimers increasing with concentration, might indicate dynamic equilibrium. This is further explored below.

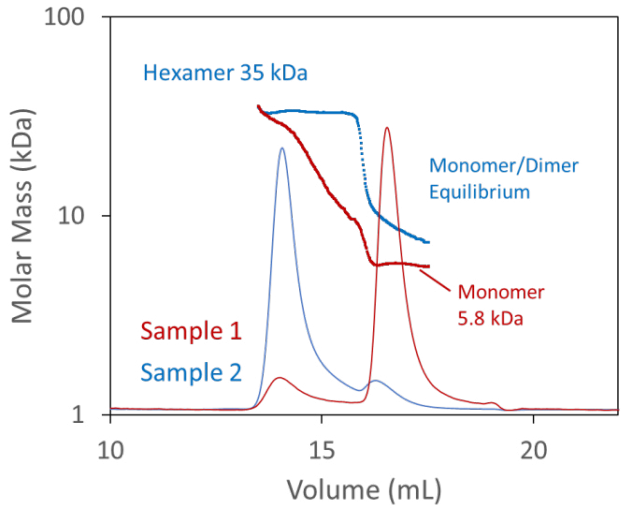

Figure 2: Plot of molar mass vs. time of Samples 1 and 2 (monomer, dimer, hexamer). The UV signal @ 280 nm is plotted as an overlay.

Further addition of zinc, in Sample 3, completely shifts the equilibrium towards the hexamer, as seen in Figure 3. In sample 3 another molecular species is detected which is identified as the dodecamer of the insulin molecule. It shows a molar mass of 70 kDa and, although present only in a small amount, generates a distinct signal clearly observed in by the LS detector.

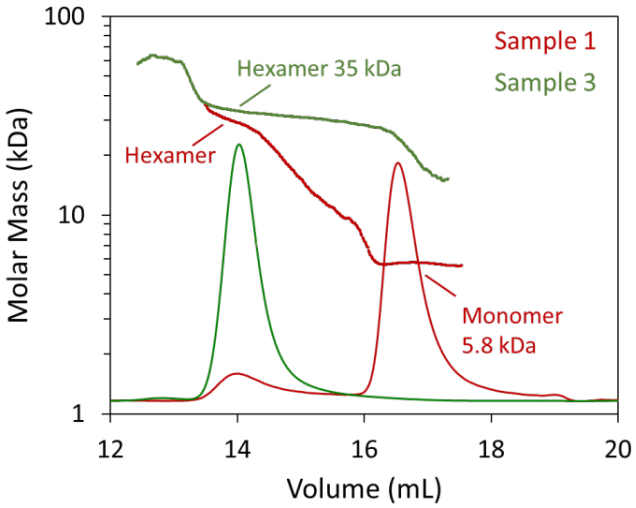

Figure 3: Plot of molar mass vs. time of Samples 1 and 3. The UV signal @ 280 nm is plotted as an overlay.

Concentration effects

SEC-MALS allows the determination of self-association tendencies. The effect of injection volumes on the sample was investigated, i.e. 50 and 200 µL of the same sample solution was injected to the SEC-MALS. Since the peak width is approximately constant, increasing the injection volume results in higher peak concentrations, facilitating the identification of fast dynamic equilibria.

The increase of injected volume clearly affects the equilibrium of Sample 2 (Figure 4). As a higher insulin concentration is achieved, the equilibrium of the monomer-dimer is shifted towards dimer. The smallest species observed when 50 µL is injected is monomer while the corresponding smallest species is dimer when 200 µL is injected. The hexamer fraction is unaffected and shows no tendency to form larger oligomers.

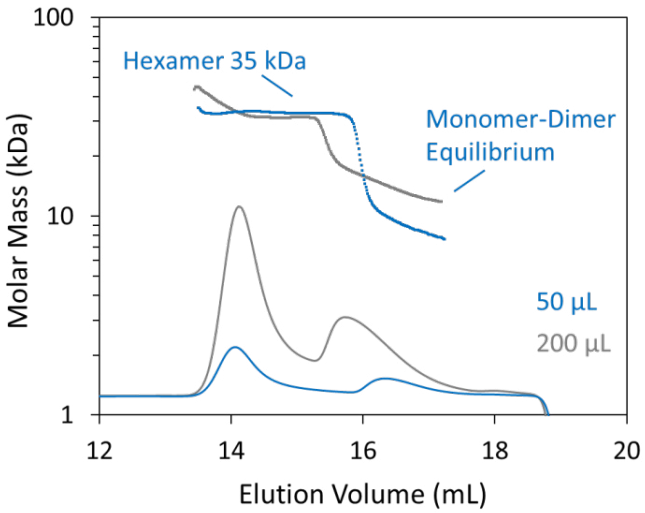

Figure 4: Plot of molar mass vs. time of Sample 2. The UV signal @ 280 nm is plotted as an overlay.

In the case of Sample 3 there are basically no effect of varying the injection volume (Figure 5). In presence of 0.3 mM zinc the system is "locked" on hexamer and identical molar masses are detected at both concentrations (50 and 200 µL injected). Obviously, the self-association behavior of the hexamer is significantly different from that of the monomer.

Conclusions

Multi-angle light scattering proves to be the method of choice for the examination of association phenomena not only for large proteins such as antibodies, but also for peptide molecules with lower molecular masses. Since the use of proteins and peptides for therapeutic purposes is permanently increasing, the application of light scattering as a powerful method of molecular characterization will also become more and more important.

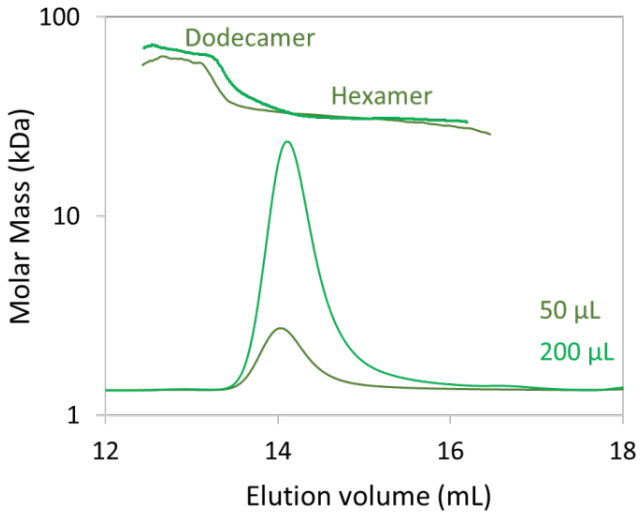

Figure 5: Plot of molar mass vs. time of Sample 3. The dRI signal is plotted as an overlay (the UV signal is saturated due the high sample load).

References

1. Attri A.K., Fernández C., Minton A.P. pH-dependent self-association of zinc-free insulin characterized by concentration-gradient static light scattering. *Biophys. Chem.* **148**, 28-33 (2010).
2. Attri A.K., Fernández C., Minton A.P. Self-association of Zn-insulin at neutral pH: Investigation by concentration gradient-static and dynamic light scattering. *Biophysical J.* **148**, 23-27 (2010).
3. Ludwig D.B., Webb J.N., Fernandez C., Carpenter J.F., Randolph T.W. Quaternary Conformational Stability: The Effect of Reversible Self-Association on the Fibrillation of Two Insulin Analogs. *Biotechnology and Bioengineering* **108**, 2359-2370 (2011).
4. Jensen M. H., Wahlund P.-O., Jacobsen J. K., Vestergaard B., van de Weert M., Havelund S. Self-association of long-acting insulin analogues studied by size exclusion chromatography coupled to multi-angle light scattering. *J. Chromatography B* **879**(28), 2945-2951 (2011).
5. Jonassen I., Havelund S., Hoeg-Jensen T., Steensgaard D. B., Wahlund P.-O., Ribel U. Design of the Novel Protraction Mechanism of Insulin Degludec, an Ultra-long-Acting Basal Insulin. *Pharm. Res.* **29**(8), 2104-2114 (2012).

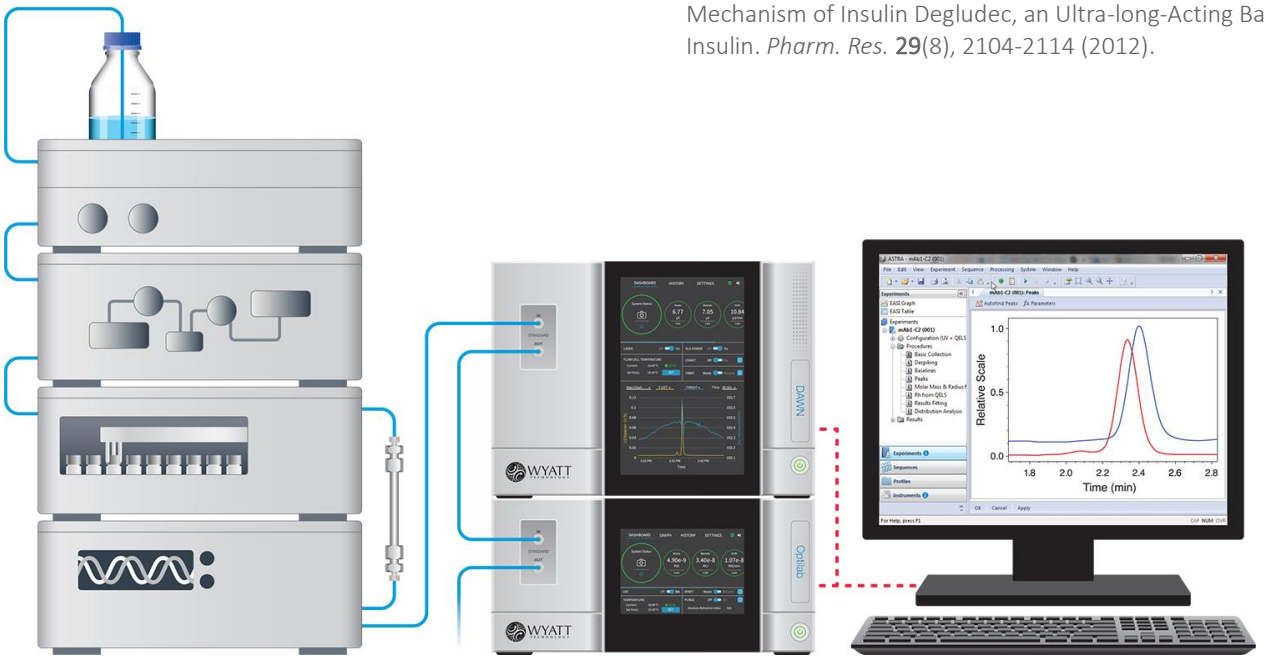

WYATT TECHNOLOGY

APPLICATION NOTE

AN5005: Characterization and Formulation Screening of mAb and Antibody-Drug Conjugates (ADCs) by High-throughput DLS

Aileen La, Ananda Seneviratne, Gaya Ratnaswamy, Jihea Park
Agensys, Inc., an affiliate of Astellas Pharma

Summary

Antibody-drug conjugates (ADCs) are important biotherapeutic candidates that combine highly potent cytoxic drugs with monoclonal antibodies (mAb) for targeted drug delivery in the treatment of cancer or neurodegenerative disorders. However, while the underlying mAb may be a relatively stable molecule, the addition of the drug and linker often destabilizes the protein or adds undesirable intermolecular interactions, so that ADC biotherapeutics are heavily prone to aggregation. Uncontrolled aggregation can lead to a loss in clinical efficacy in vivo or, in extreme cases, invoke a serious immunogenic response. Monitoring stability during formulation is therefore essential to ensure that ADC compounds meet commercial, performance and safety targets.

This application note demonstrates how high-throughput dynamic light scattering (DLS) with automated well-plate sampling using the DynaPro® Plate Reader and DYNAMICS® software enables the rapid and reliable characterization of two ADCs based on monoclonal antibodies (mAb) IgG1 and IgG2. The results show that the attachment of small molecule drugs to the mAb does not appreciably change the molecule's average size (hydrodynamic radius, R_h). However, polydispersity slightly increases, indicating the presence of some high molecular weight species in this region.

Data are also presented to illustrate the use of DLS in formulation screening. Trend studies into pH, temperature and buffer variations show that the automated DynaPro Plate Reader is an effective tool for rapid, high-throughput biotherapeutic screen.

Introduction

Antibody drug conjugates (ADCs), also known as immunoconjugates, are a novel class of biotherapeutics which combine IgG1 and IgG2 monoclonal antibodies (mAb) with small molecular cytotoxic drugs, such as maytansines, auristatins, duocarmycin or calicheamicin. Several ADC-based drugs are currently available for targeted cancer treatment, with many more undergoing clinical trials.

Figure 1. Automated DLS with the DynaPro Plate Reader improves productivity in formulation stability studies.

ADC product development presents a complex formulation challenge in comparison to standard monoclonal antibody drugs. As more small-drug molecules are attached to the mAb base the conjugate becomes increasingly hydrophobic, which may compromise critical performance attributes such as solubility and physical stability. Monitoring and controlling the behavior of the ADC complex in formulation is therefore essential to ensuring the drug meets pharmacological, safety and commercial performance targets.

Dynamic Light Scattering (DLS) is one of the most effective techniques for submicron size analysis of proteins, their aggregates and other nanoparticles. DLS provides rapid measurements of hydrodynamic radius (R_h), degree of polydispersity, temperature of aggregation onset, and colloidal stability. Formulation screening with DLS helps developers rationalize variables such as temperature, pH or concentration in terms of their impact on stability, solubility or propensity to aggregate. Identifying the biological target and formulation conditions most likely to deliver ideal behavior during early phase screening accelerates the development process and greatly reduces the risk of downstream failure.

Traditional DLS measurements are performed in batch mode, making formulation analysis a time- and labor-intensive process. Advances in DLS technology have greatly increased the productivity of formulation screening while maintaining the high performance and accuracy demanded by industry, by performing automated, high-throughput DLS analysis in situ in standard 96-, 384- or 1536-well microtiter plates. In this study, the hydrodynamic radii and physical stability of samples of IgG1, IgG2 and ADCs based on those molecules were measured using the DynaPro Plate Reader high-throughput DLS system under a variety of formulation conditions.

Materials and Methods

Monoclonal antibodies (IgG1 and IgG2, expressed in two different cell lines) and antibody drug conjugates (IgG1-Drug 1 and IgG2-Drug 1) were characterized using DLS. The R_h, polydispersity (%Pd), and presence of any high molecular weight species in solution were measured. Regularization analysis was performed to determine R_h, %Pd and the relative mass of the fitted peaks.

A 20–70 µL sample volume was used at a concentration of 1.0 mg/mL. Prior to sample analysis, the well-plate was centrifuged at 3000 rpm for 1 minute to remove air bubbles. Each sample was measured in triplicate in which a single measurement consists of 10 acquisitions for 10 seconds at 25°C. The raw data (auto-correlation functions) was analyzed by cumulants analysis and/or regularization analysis. The distribution plots were obtained from regularization analysis.

Instrumentation

The data were acquired at 25°C using the temperature-controlled DynaPro Plate Reader and DYNAMICS software. A 384-well plate was used to enable automated, high-throughout sample analysis.

Results and Discussion

Figure 2 shows the dispersion plots and histograms for mAb 1a and mAb 1b (IgG1) and mAb 2 and mAb 3 (IgG2). The results are tabulated in Table 1.

DLS analysis shows that that IgG1 and IgG2 have almost the same R_h while IgG2 has a greater degree of polydispersity than IgG1. This may be attributed to the two additional disulfide bonds present in IgG2 which often lead to greater heterogeneity.

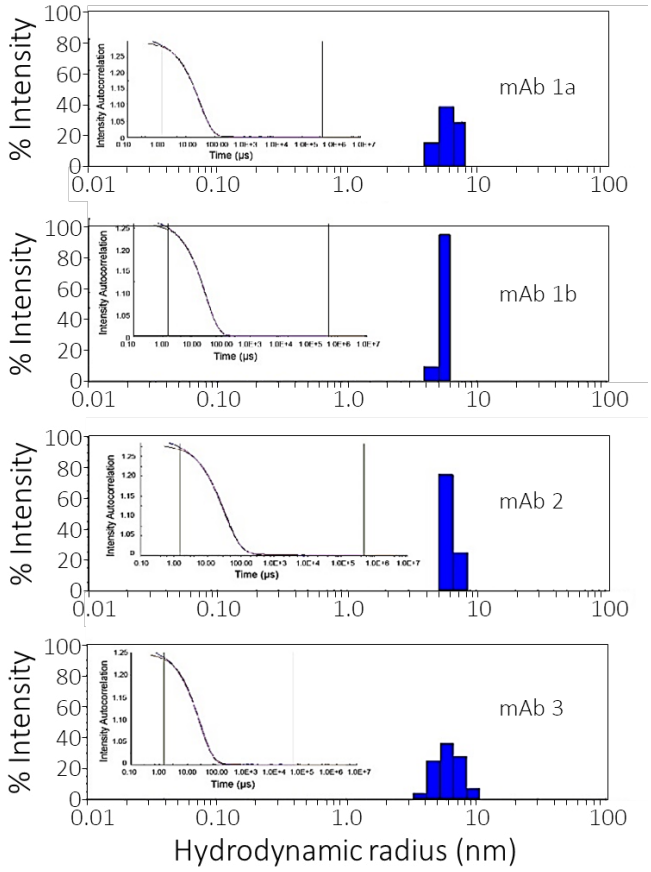

Figure 2. The autocorrelation functions and regularization histograms of mAb 1a, mAb1b (IgG1) vs. mAb 2 and mAb 3 (IgG2).

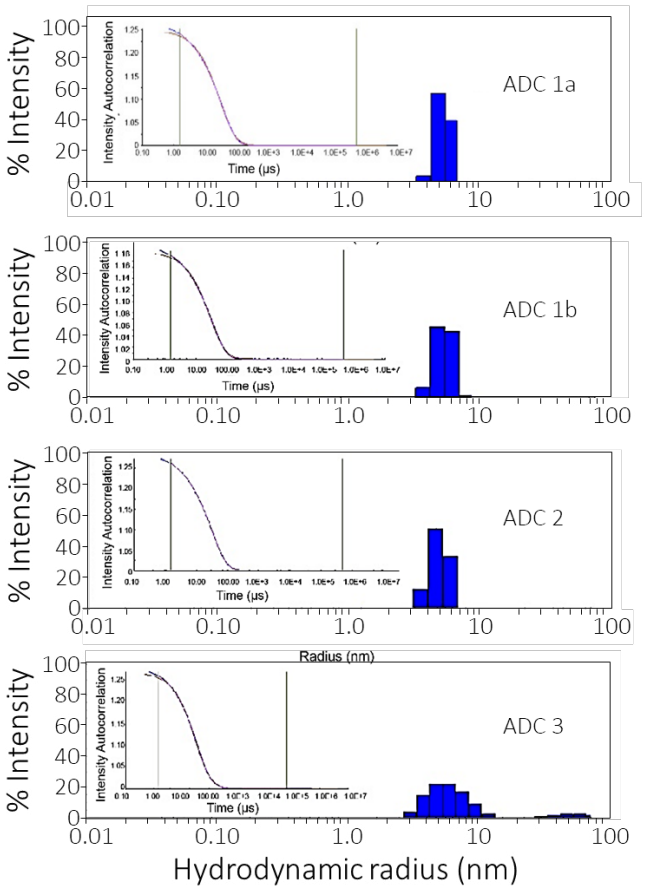

Figure 3 The autocorrelation functions and regularization histograms of ADC 1a, ADC1b (IgG1) vs. ADC2 and ADC3 (IgG2).

Table 2 and Figure 3 provide a comparison of corresponding IgG1 vs. IgG2 ADC in the recommended lead formulations. A sample exhibiting %Pd < 20% is generally considered to be monodisperse. Therefore, a measured level of polydispersity beyond 20% indicates heterogeneity within the sample. The data suggest that although attachment of the small molecule drug to the mAb does not change R_h, the ADC samples become more polydisperse than the mAb samples. Hydrophobicity also increases slightly, indicating the presence of some high molecular weight species.

Formulation Screening

Four mAb formulations were screened using automated DLS to determine their behavior under different conditions. Figure 4 shows how R_h and %Pd of the proteins vary as pH is incrementally increased while temperature remains within the range of 2-8°C. At pH 5.5 %Pd falls to 11.4 indicating that the sample is mostly monodisperse with less proteins present in the higher molecular weight region.

Table 1. The hydrodynamic radii and polydispersities of IgG1 vs. IgG2, calculated by two different methods.

	Type	mAb 1a IgG1	mAb 1b IgG1	mAb 2 IgG2	mAb 3 IgG2
Cumulants	Average R_h(nm)	5.3	5.3	5.6	5.0
	% Pd	15.3	13.4	25.7	21.5
	Main Peak R_h (nm)	6.1	6.0	6.7	6.2
Regularization	Main Peak Mass, %	100.0	100.0	99.6	100.0
	Main % Pd	21.6	18.0	31.6	27.3

Table 2. The DLS data of ADC: IgG1 (mAb1a-ADC and mAb1b-ADC) vs IgG2 (mAb2-ADC and mAb3-ADC).

	Type	mAb1a-ADC (ADC1a)	mAb1b-ADC (ADC1b)	mAb2-ADC (ADC2)	mAb3-ADC (ADC3)
Cumulants	Average R_h (nm)	5.6	7.2	5.2	6.5
	%Pd	15.7	30.8	23.5	34.5
	Main Peak R_h (nm)	6.5	7.4	6.9	8.0
Regularization	Main Peak Mass, %	99.4	99.6	100.0	100.0
	Main %Pd	21.6	18.0	32.3	33.9

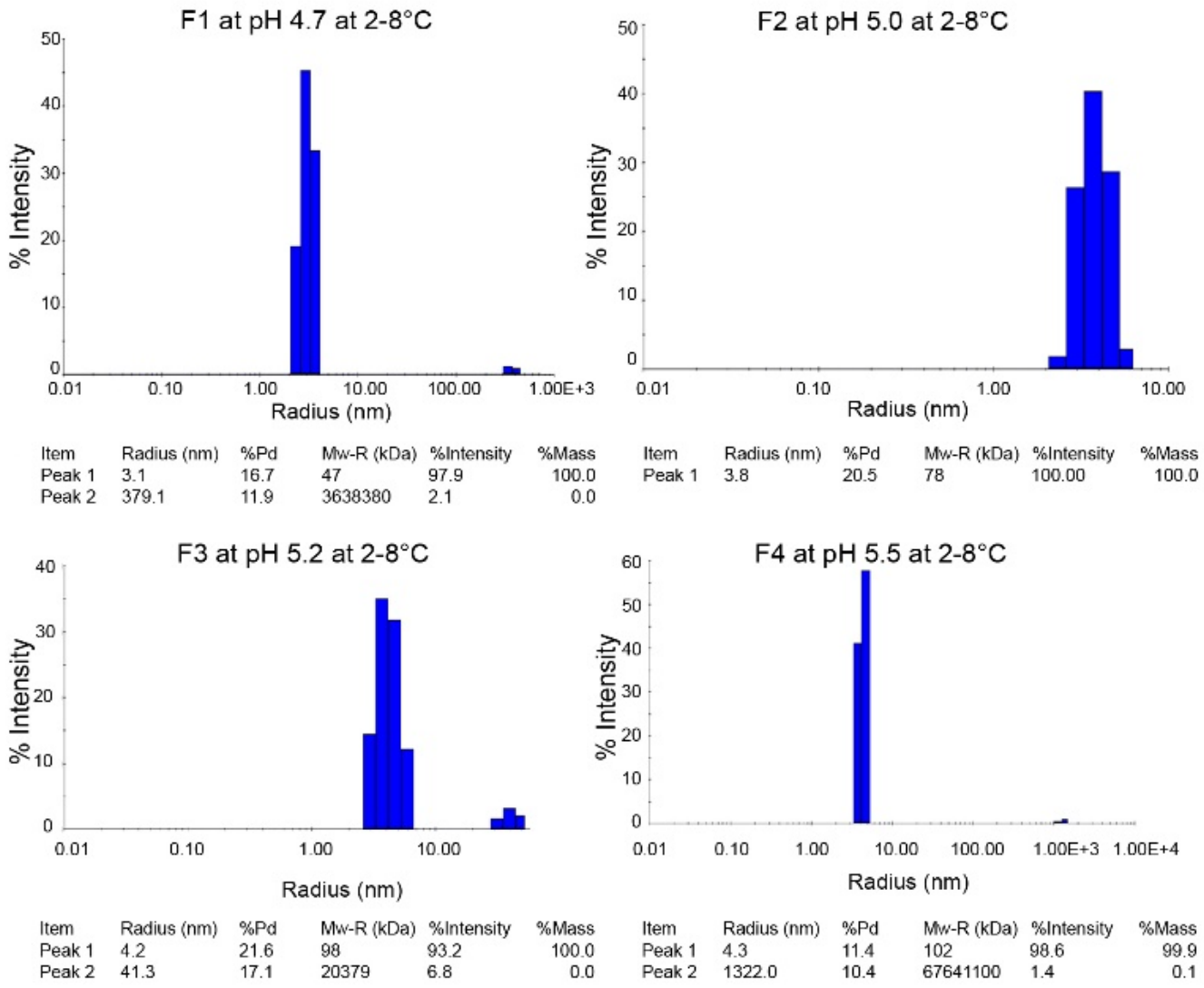

Item	Radius (nm)	%Pd	Mw-R (kDa)	%Intensity	%Mass
Peak 1	3.1	16.7	47	97.9	100.0
Peak 2	379.1	11.9	3638380	2.1	0.0

Item	Radius (nm)	%Pd	Mw-R (kDa)	%Intensity	%Mass
Peak 1	3.8	20.5	78	100.00	100.0

Item	Radius (nm)	%Pd	Mw-R (kDa)	%Intensity	%Mass
Peak 1	4.2	21.6	98	93.2	100.0
Peak 2	41.3	17.1	20379	6.8	0.0

Item	Radius (nm)	%Pd	Mw-R (kDa)	%Intensity	%Mass
Peak 1	4.3	11.4	102	98.6	99.9
Peak 2	1322.0	10.4	67641100	1.4	0.1

Figure 4. DLS Histograms of R_h for four mAb formulations at different pH values.

Figure 4 shows that R_h increases with pH. The shift can be attributed to increased electrostatic repulsion at higher pH. Additionally, a temperature trend study shows that at pH 5.5 the antibodies are relatively stable with a slight increase in R_h around 40 ℃.

Finally, eight ADC formulations were analyzed in different histidine (F1-F5) and citrate (F6-F8) buffer solutions (Table 3). Figure 5 shows that proteins in three citrate formulations (F6-F8) are more polydisperse, with higher R_h than the histidine formulations. Overall, these data suggest that F5 at pH 5.3 with R_h of 6 nm and %Pd of 4.2% is the most stable formulation.

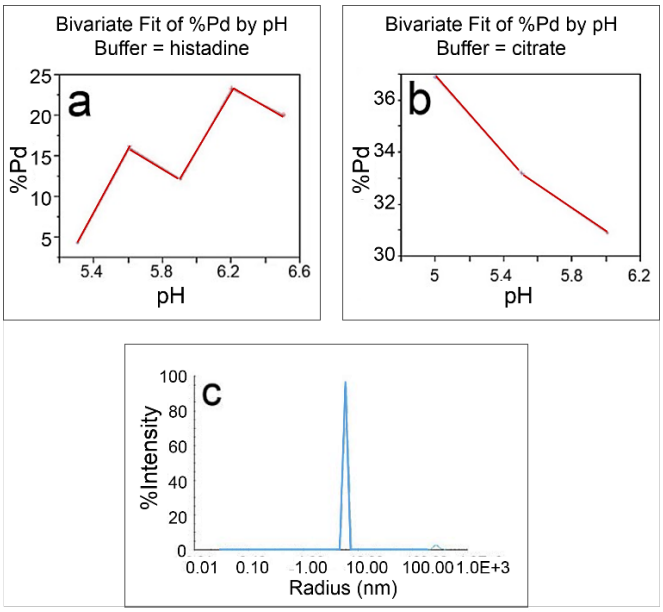

Figure 5. Formulation screening: %Pd of histidine formulations (a) vs. citrate formulations (b) and the histogram of the F5 formulation (c).

Conclusions

DLS is a rapid and useful bioanalytical method for biotherapeutic characterization and formulation screening. By providing R_h and polydispersity measurements over a series of conditions, DLS enables developers to closely monitor and control the stability of their formulation throughout every stage of the development process. Additional studies may be carried out to determine the thermal and colloidal stability profiles of each candidate and buffer condition.

High-throughput screening of formulations and drug candidates is made possible by the DynaPro Plate Reader. This instrument reduces the labor intensity and cost of investigative trend studies through automation and its unique ability to carry out DLS measurements in situ in microtiter plates.

Table 3. DLS data of eight ADC formulations in Histidine (F1-F5) and citrate buffers (F6-F8). These data suggest that proteins in formulation F5 are the most stable.

Formulation ID	Buffer Type	pH	R_h	%Pd	%Mass
F1	histadine	6.5	5.985	20.0	99.8
F2	histadine	6.2	6.056	23.3	99.8
F3	histadine	5.9	5.526	12.1	99.9
F4	histadine	5.6	5.448	16.0	99.7
F5	histadine	5.3	5.931	4.2	99.6
F6	citrate	5.0	8.338	36.9	99.8
F7	citrate	5.5	8.084	33.2	99.8
F8	citrate	6.0	7.818	30.9	99.5

APPLICATION NOTE

AN3009: Characterization of self-associating antibody solutions at high concentrations with CG-MALS

Sophia Kenrick, Ph.D. and Daniel Some, Ph.D., Wyatt Technology Corp.

Summary

The characterization of therapeutic protein formulations is essential for the development of novel biopharmaceuticals. In particular, solution viscosity and colloidal stability may be adversely impacted by attractive self-interactions among protein molecules. In this study, we quantified the self-association affinity and stoichiometry of three antibody formulations (mAbs A, B, and C) in their corresponding formulation buffers using composition-gradient multi-angle light scattering (CG-MALS).

Experiments were performed with a Calypso® concentration-gradient system, a DAWN® multi-angle light scattering (MALS) detector, and Optilab® dRI detector with high concentration range (HC model). The Calypso automated the generation of 8-9 concentrations of each antibody up to concentrations ~40 mg/mL and delivered them to downstream detectors. Additional measurements of higher concentrations were made with a microCuvette®. The light scattering and concentration data were collected with the CALYPSO™ software and fit to an appropriate interaction model, taking into account both specific attractive interactions and nonspecific repulsive interactions, expressed as a positive second virial coefficient, A_2.

The viscosity of the antibody stock solutions correlated well to the measured attractive interactions among the molecules. The lowest viscosity formulation (mAb A) exhibited only repulsive interactions, quantified by a second virial coefficient of 7.3×10^{-5} mol·mL/g^2 which is slightly more repulsive than the pure excluded-volume A_2 of ~5.0×10^{-5} mol·mL/g^2. In contrast, mAbs B and C exhibited significant self-association; the best fit to the light scattering data indicated that the antibodies form weak dimers, which associate further to form higher order oligomers. This self-association is believed to be the mechanism behind increased viscosity at the formulation concentration.

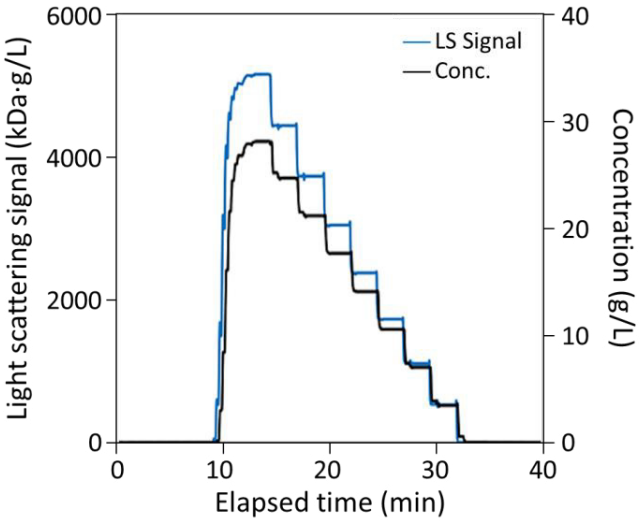

Typical light scattering and measured concentration for CG-MALS gradient automated by the Calypso.

	A_2 (mol·mL/g^2)	Dimerization K_D (μM)	ISA K_D (μM)
mAb A	7.13×10^{-5}	--	--
mAb B	4.47×10^{-5}	280	180
mAb C	5.09×10^{-5}	400	130

Best fit parameters for self-interactions of mAbs A, B, and C. Samples B & C exhibit transient association forming fairly large oligomers.

Introduction

Recent research suggests that weak protein-protein interactions play a key role in the viscosity and colloidal stability of a protein formulation[1]. Batch (unfractionated) multi-angle light scattering (MALS) is uniquely suited to quantifying these interactions, enabling measurements in solution at the concentration of interest without tagging, immobilization, or other sample modifications[2,3]. In this study, we applied automated composition-gradient multi-angle light scattering (CG-MALS)[4] to the characterization of the intermolecular interactions of three antibody formulations to evaluate the correlation of these interactions with the formulation viscosity.

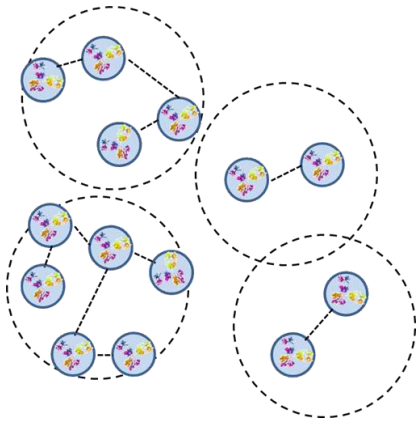

Figure 1: Antibody molecules associate with nearest neighbors into loose networks described as quasi-specific oligomers.

Materials and Methods

Antibody and buffer solutions were kindly provided by MedImmune, LLC (Gaithersburg, MD). Light scattering data for each antibody was measured in its respective formulation buffer at 15-20 concentrations. For mAb A, all dilutions were automated by the Calypso. For mAbs B and C, some dilutions were performed manually and measured using a microCuvette.

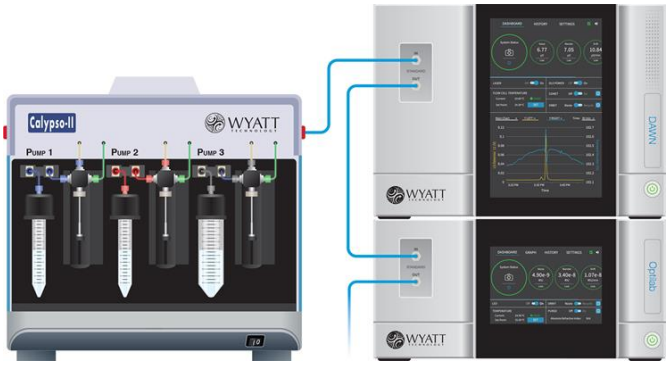

Automated CG-MALS Measurements

For the automated Calypso measurements, mAb formulations were first diluted in their formulation buffer 2- 5x and filtered to 0.02 µm; the resulting concentrations are given in Table 1. Automated composition gradients were performed using a Calypso, a DAWN MALS detector with laser power reduced to 50% to prevent signal saturation, and an Optilab refractive index detector with high concentration option. For each composition, the Calypso mixed an aliquot of antibody and buffer and delivered it to the downstream LS and concentration detectors and stopped the flow for 60 seconds. Pump control, data acquisition and analysis were all performed by the CALYPSO software. A typical Calypso method is shown in Figure 2.

	Viscosity (cP)		Max. Conc. for Calypso (mg/mL)
mAb A	~3	(at 100 mg/mL)	43
mAb B	~7	(at 100 mg/mL)	32
mAb C	~13	(at 150 mg/mL)	28

Table 1: Antibody properties and initial dilution for automated measurements

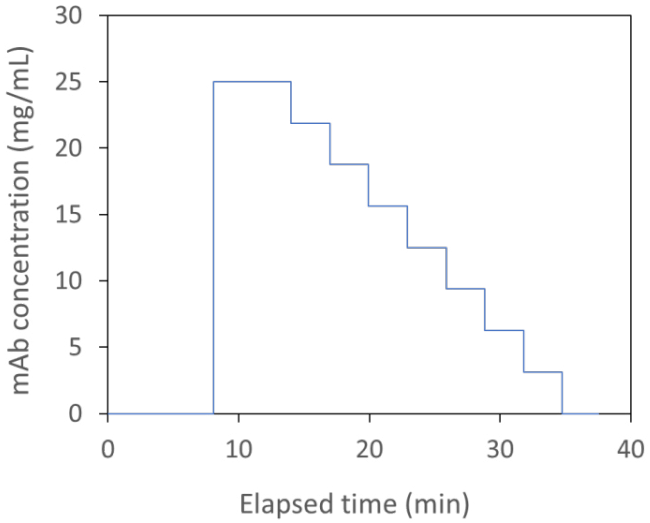

Figure 2: Automated Calypso composition gradient. At each step, the Calypso injected antibody solution at the desired concentration and stopped the flow for 60 seconds to allow for any dissociation kinetics.

Manual microCuvette Measurements

At the highest concentrations required, the viscosity of mAbs B and C exceeded the capacity of the Calypso. In order to collect additional high concentration data,

dilutions were prepared manually, and light scattering was measured by the DAWN in a microCuvette. mAb A was also measured in this manner for comparability purposes. In preparation for these experiments, mAb A was filtered to 0.1 µm and mAbs B and C were filtered to 0.2 µm. Dilutions of the filtered stock solution were made with buffer filtered to 0.02 µm. To prevent saturation of detector signals at the highest concentrations, the DAWN's laser power was set to 100% for mAb A, 13% for mAb B, and 25% for mAb C.

Results and Discussion

The difference in intermolecular interactions between the three antibodies is immediately apparent in their light scattering data. Although all three molecules have a monomer molecular weight ~150 kDa, the LS signals for mAbs B and C exhibit a significantly different behavior than that of mAb A under the same concentrations (Figure 3). In fact, at ~100 mg/mL, the light scattering signal from mAbs B and C is ~8.5-fold that of mAb A. This indicates that mAbs B and C exhibit strong attractive interactions, compared to mAb A. It is plausible to assume that these attractive interactions are the mechanism for their increased viscosity.

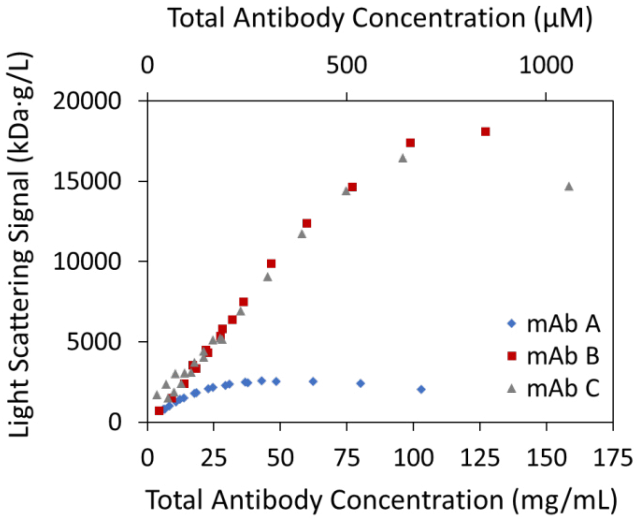

Figure 3: Light scattering signal as a function of concentration for monoclonal antibodies A, B, and C

Data analysis of mAb A, which exhibited the lowest viscosity, indicates no attractive self-interactions. Rather, mAb A experienced only repulsive interactions, quantified by a second virial coefficient A_2 = 7.3x10^{-5} mol·mL/g^2. This is equivalent to the excluded volume interactions exhibited by a hard sphere with molecular weight 150 kDa and radius 5.5 nm. The effective radius is slightly larger than the actual hydrodynamic radius of IgG (which is generally in the range of 4.8 – 5.2 nm as determined by dynamic light scattering), suggesting additional intermolecular repulsion due in all likelihood to partially screened charge-charge repulsion. We note here that while only A_2 is reported, the analysis actually allows for a sixth-order virial expansion where all virial coefficients are calculated from a single free parameter, the hard-sphere specific volume.

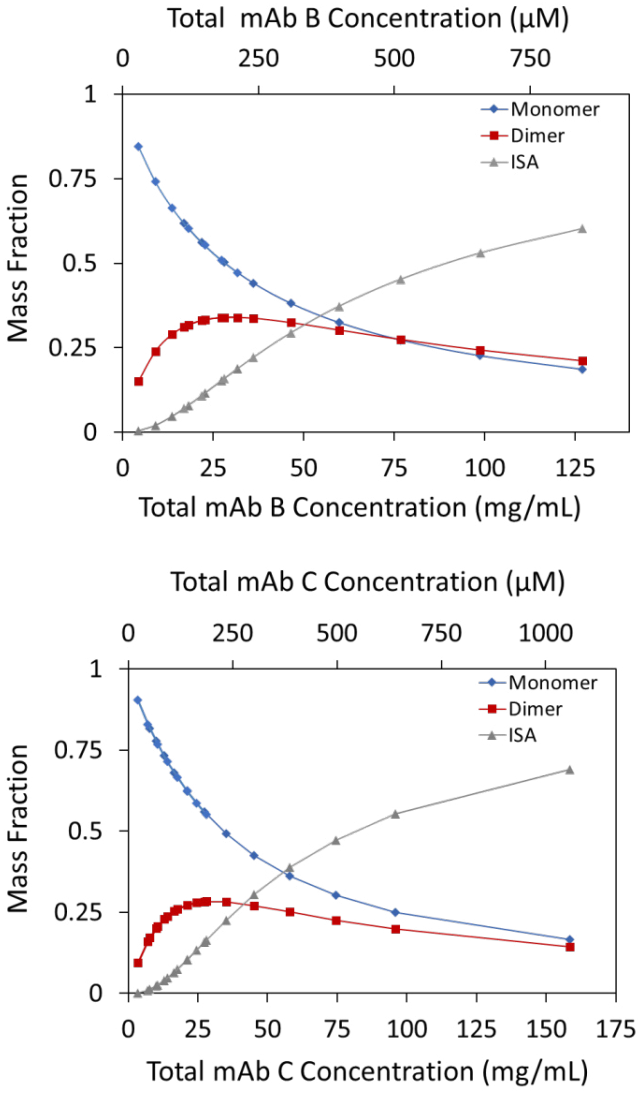

Figure 4: Mass distribution of oligomeric species for mAb B (top) and mAb C (bottom) as derived from fitting the light scattering data vs. concentration to a model that included an equilibrium between monomers, dimers, and infinite self-association (ISA) of dimers. The "ISA" (▲) curves refer to the mass fraction of all n-mers, where n = 4, 6, 8...

In contrast, both mAbs B and C appeared to form clusters or loose networks of quasi-specifically associated oligomers (Figure 1). Even in the dilute experiments performed with automated concentration gradients, the apparent molecular weight indicated oligomerization into species with at least dimer molecular weight. After concatenating the data sets obtained in both (lower concentration) automated Calypso-generated gradients and (higher concentration) manual cuvette measurements, several association models were considered for each antibody. As a first pass, the data were fit to models that incorporated dimers, trimers, etc. with arbitrary, independent association constants. Then the model was refined for a particular mechanism of self- association.

In the case of mAb C, the best fit required n-mers with n>6. In addition, the curvature in the LS data as a function of concentration was fit best when odd-numbered oligomers were omitted. For this antibody, the best fit to the data was finally accomplished with a model that assumes the following: 1) antibody monomers formed dimers (mAb_2) with affinities "Dimerization K_d" on the order of several hundred micromolar; 2) these dimers further self-associated to form higher-order oligomers ($(mAb_2)_n$) with an independent affinity "ISA K_d". The dimer-dimer interaction is calculated according to a model of isodesmic, infinite self-association (ISA) wherein each dimer adds to the progressively assembled chain or cluster with equal affinity[5].

The equilibrium dissociation constants are listed in Table 2. Based on the calculated affinities, mAb C appears to exhibit a small degree of cooperativity: the affinity of dimer-dimer association ("ISA K_d") is higher than that of monomer-monomer ("Dimerization K_d"). Though the difference between the two affinities is not great, it is significant within experimental and fitting error. This phenomenon is not unusual and has been considered previously in terms of nucleation models of association [see Reference 5 and references therein].

The same dimer/ISA model also yielded the best fit to the data when applied to mAb B. Figure 4 shows the mass distribution of monomer, dimer, and higher order oligomers (ISA) for each antibody. Based on this model, the molar distribution of each oligomer could be calculated, and for both mAbs B and C, oligomers >10-mers represented <1% mol/mol.

One point of distinction between the two antibodies is the lack of statistically significant difference in mAb B's Dimerization K_d and ISA K_d values. A second point is the viable alternative description of the interactions among mAb B molecules as an isodesmic self-association of monomers (rather than an association of dimers), i.e., monomer mAbs self-assemble progressively with each monomer adding to the growing oligomer with equal affinity (K_d = 430 µM). As shown in Figure 5, a model of isodesmic self-association up to 10-mers, though not as good a fit as the dimer self-association scheme, may also be suitable for describing mAb B (dashed red line, Figure 5); however, this model clearly does not agree with the data collected for mAb C. Additional data with mAb B at ~160 mg/mL would be required to confirm the association model.

	A_2 (mol·mL/g^2)	Dimerization K_d (µM)	ISA K_d (µM)
mAb A	7.13×10^{-5}	--	--
mAb B	4.47×10^{-5}	280	180
mAb C	5.09×10^{-5}	400	130

Table 2: Best fit parameters for self-interactions of mAbs A, B, and C

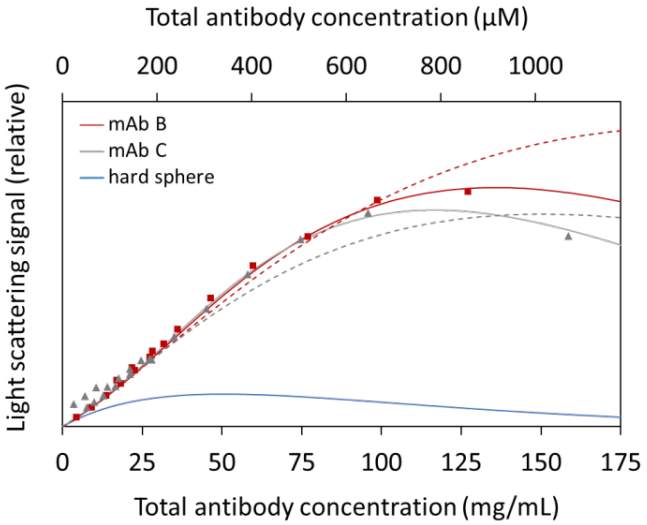

Figure 5: Light scattering data for mAbs B and C best fit to a model of infinite self-association of dimers (solid line) or isodesmic self-association of monomers (dashed line). A model of typical excluded volume repulsion, with no attractive interactions, (e.g., mAb A) is shown for reference.

In addition to the attractive interaction, thermodynamic non-ideality must be taken into account in the form of a

positive second virial coefficient. Here, A_2 quantifies only the portion of the interaction due to nonspecific repulsion, such as excluded volume and charge-charge repulsions. The A_2 values for mAbs B and C were similar (Table 2), and were equivalent to the excluded volume interactions exhibited by a hard sphere with molecular weight 150 kDa and radius 4.7-4.8 nm.

Conclusions

CG-MALS measurements automated by the Wyatt Calypso provided insight into the mechanism behind the different colloidal behaviors of three antibody solutions. Analysis of CG-MALS data via the CALYPSO software quantified both the attractive and repulsive interactions. The net attractive interactions in formulations B and C correlated to their increased viscosity as compared to mAb A, illuminating the nature of the intermolecular forces that contribute to high viscosity.

For more information on Calypso, please visit www.wyatt.com/Calypso.

To learn more about CG-MALS see www.wyatt.com/CG-MALS.

References

1. Minton, A. P. Static Light Scattering from Concentrated Protein Solutions, I: General Theory for Protein Mixtures and Application to Self-Associating Proteins. *Biophys. J.* **93**, 1321–1328 (2007).
2. Scherer, T. M., Liu, J., Shire, S. J. & Minton, A. P. Intermolecular Interactions of IgG1 Monoclonal Antibodies at High Concentrations Characterized by Light Scattering. *J. Phys. Chem. B* **114**, 12948–12957 (2010).
3. Some, D. & Kenrick, S. Characterization of Protein-Protein Interactions via Static and Dynamic Light Scattering. *Protein Interact.* (2012) doi:10.5772/37240.
4. Yadav, S., Liu, J., Shire, S. J. & Kalonia, D. S. Specific interactions in high concentration antibody solutions resulting in high viscosity. *J. Pharm. Sci.* **99**, 1152–1168 (2010).
5. Zehender, F., Ziegler, A., Schönfeld, H.-J. & Seelig, J. Thermodynamics of Protein Self-Association and Unfolding. The Case of Apolipoprotein A-I. *Biochemistry* **51**, 1269–1280 (2012).

WYATT TECHNOLOGY

WYATT TECHNOLOGY

APPLICATION NOTE

AN3004: Self-association of insulin quantified by CG-MALS

Vijay Pandyarajan, M.D., Ph.D.[1], Nelson B. Phillips, Ph.D.[1], Sophia Kenrick, Ph.D.[2], Michael A. Weiss, Ph.D.[1]
[1]Case Western Reserve University [2]Wyatt Technology Corp.

Summary

Therapeutic insulin analogs, engineered for specific states of self-association, have revolutionized the treatment of diabetes mellitus. Modifications that impact the self-association of these molecules in turn alter their pharmacokinetics and pharmacodynamics, resulting in fast-acting drugs best suited for prandial regimens and insulin pumps or extended-release versions for once daily dosage[1]. Hence the ability to quantify the affinity and stoichiometry of insulin self-association is central to developing efficacious analogs.

In this note, we quantify the self-association of insulin at neutral pH in the absence of Zn^{2+} using composition-gradient multi-angle light scattering (CG-MALS). CG-MALS enables rapid, reproducible, label-free quantification of biomolecular self-association. The increase in weight-average molar mass as a function of concentration is fit to an appropriate association model to yield the absolute stoichiometry and affinity of the interactions.

Under these conditions, insulin undergoes isodesmic self-association. Monomers self-associate to form dimers, trimers, and all higher order complexes. Each monomer adds to the growing cluster with equivalent affinity, in this case K_d = 52 µM. At the maximum concentration tested (3.2 mg/mL, 536 µM), an adequate description of the insulin solution must include oligomers >10-mer.

Introduction

Composition-gradient multi-angle light scattering (CG-MALS) has been previously applied to quantify the self-association of macromolecules in solution, including insulin[1-5]. In the presence of Zn^{2+}, insulin forms native hexamers that further self-associate into higher order structures[2]. In the absence of Zn^{2+}, however, insulin monomers associate according to an isodesmic model, with each monomer adding to the growing cluster with equal affinity[3].

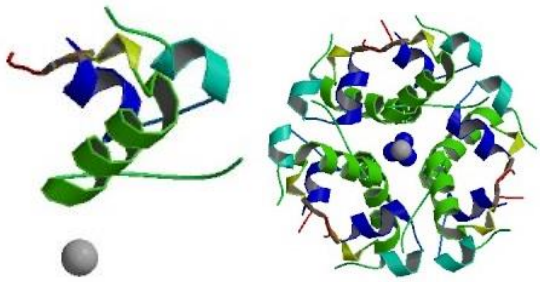

Figure 1: Crystal structure of insulin monomer (left) and hexamer (right) in the presence of zinc, PDB ID: 1TRZ

Materials and Methods

Human insulin samples were prepared in a buffer containing 20 mM sodium phosphate pH 7.2, 0.1 M NaCl, 1 mM EDTA and quantified using an extinction coefficient of 1.05 AU/(g/L*cm) at 276 nm. Insulin solutions and buffers were immediately filtered using Anotop 0.02 µm pore size syringe filters and degassed by centrifugation at 2500 g for 15 minutes. Experiments were performed at 25°C in duplicate using two stock concentrations of either 3.2 mg/ml or 0.3 mg/ml. CG-MALS experiments were performed using a Calypso® concentration-gradient system to create a concentration gradient in line with a Shimadzu SPD-6AV UV/Vis spectrometer and a miniDAWN® three-angle light scattering photometer (Figure 2). The light scattering and concentration data were fit to various self-association models using the CALYPSO™ software in order to determine the association scheme that best described the data.

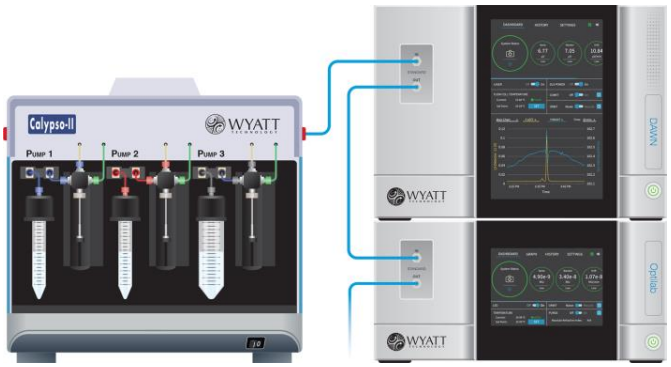

Figure 2: Calypso hardware setup

Results and Discussion

As expected, the measured light scattering and concentration data for insulin in the absence of Zn^{2+} are characteristic of a self-associating molecule (Figure 3). Although the maximum measured M_w under these conditions (38 kDa) is approximately that of the hexamer (36 kDa), the increase in molar mass cannot be described by a simple model of monomer-hexamer equilibrium $6I \rightleftharpoons I_6$ with equilibrium association constant, $K_A = [I_6]/[I]^6$. As shown in Figure 4, this type of association underestimates the measured M_w by as much as 30% for concentrations less than ~0.2 mg/mL (34 µM) and overestimates the M_w by as much as 25% for concentrations between 0.2 and 2 mg/mL (34-340 µM).

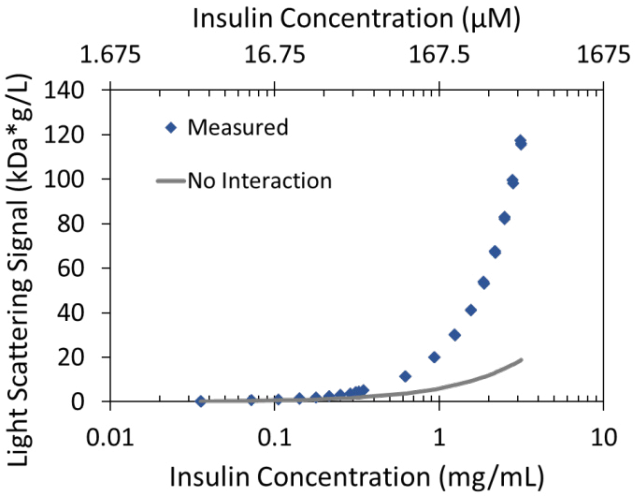

Figure 3: The measured LS signal as a function of concentration (blue diamonds) is significantly greater than the expected LS signal for a non-interacting monomer with M_w = 6 kDa (gray line).

Rather, the light scattering and concentration data are best fit by a model of isodesmic self-association. According to this mechanism, each insulin monomer adds to a growing insulin cluster with constant affinity as follows:

$$I + I \rightleftharpoons I_2 \qquad K_2 = \frac{[I_2]}{[I]^2}$$

$$I + I_2 \rightleftharpoons I_3 \qquad K_3 = \frac{[I_3]}{[I]^3} = K_2^2$$

$$\vdots \qquad \vdots$$

$$I + I_{n-1} \rightleftharpoons I_n \qquad K_n = \frac{[I_n]}{[I]^n} = K_2^{n-1}$$

The equilibrium association constant K_2 is related to the affinity per binding site, $K_d = 1/K_2$. For the data in Figure 3 and Figure 4, the best fit reveals isodesmic self-association with affinity K_d = 52 µM.

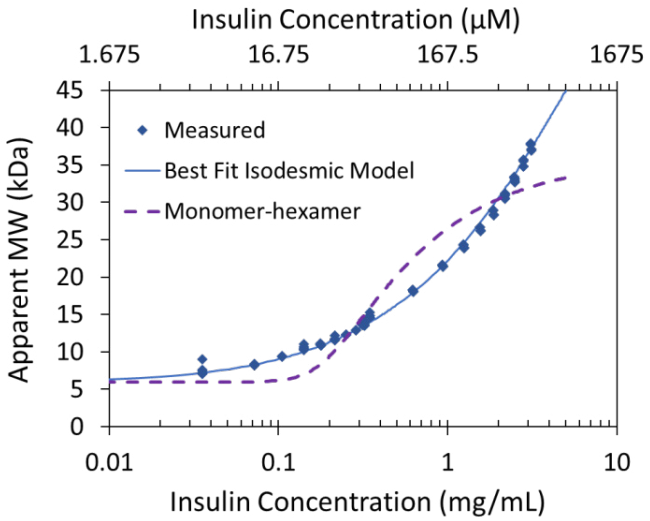

Figure 4: The increase in M_w as a function of concentration corresponds to an isodesmic self-association and is not characteristic of a simple model of monomer-hexamer equilibrium.

The equilibrium distribution of oligomers can be calculated from the self-association model (Figure 5). As the total concentration approaches the isodesmic binding site affinity (~50 µM or 0.3 mg/mL), insulin molecules self-associate, and the fraction of monomer in solution quickly decreases. At concentrations greater than ~0.6 mg/mL (~100 µM), even the contribution of dimer decreases as higher order oligomers form. At the maximum concentration (~500 µM), monomers make up only 27% mol/mol, with the remaining solution consisting of 20% mol/mol dimers and decreasing compositions of other oligomers. Figure 5 gives the molar compositions up to 15-mers, which comprise 0.3% mol/mol of the stock solution.

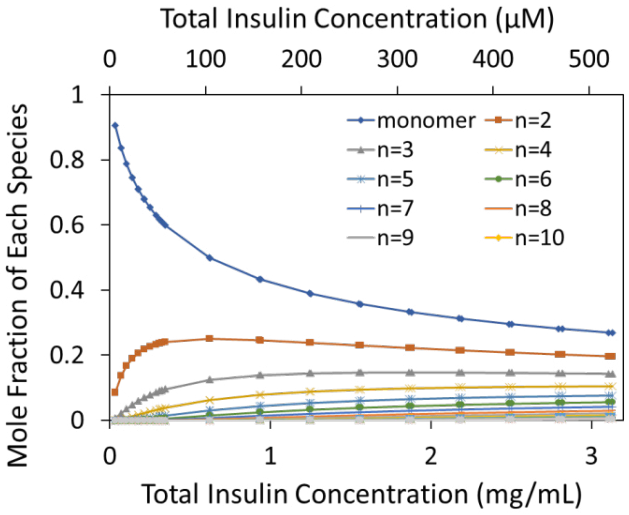

Figure 5: Equilibrium distribution of species

Conclusions

Using CG-MALS, we measured the isodesmic self-association of human insulin in the absence of zinc. According to this model, insulin monomers form dimers, trimers, and higher order oligomers, with each insulin monomer adding to the growing cluster with equal affinity, K_d = 52 µM. Although the overall M_w only changed by ~6-fold over the concentrations studied (~0.3-3 mg/mL, ~5-500 µM), the change in M_w as a function of concentration is not described by a simple monomer-hexamer equilibrium. Rather, a true description of the complexes present at equilibrium must consider higher order insulin oligomerization, with species >10-mer present under these conditions.

References

1. Berenson D.F., Weiss A.R., Wan Z.l., Weiss M.A. Insulin analogs for the treatment of diabetes mellitus: therapeutic applications of protein engineering. *Annals of the New York Academy of Sciences* **1243**(1), E40-E54 (2012).
2. Attri A.K., Fernández C., Minton A.P. Self-association of Zn-insulin at neutral pH; Investigation by concentration-gradient static and dynamic light scattering. *Biophys. Chem.* **148,** 23-27 (2010).
3. Attri A.K., Fernández C., Minton A.P. pH-dependent self-association of zinc-free insulin characterized by concentration-gradient static light scattering. *Biophys. Chem.* **148,** 28-33 (2010).
4. Some D., Kenrick S. Characterization of Protein-Protein Interactions via Static and Dynamic Light Scattering in *Protein Interactions* ed. Cai, J. and Wang, R.E. 401-426 (InTech, 2012).
5. Some D. Light-scattering-based analysis of biomolecular interactions. *Biophys. Rev.* **5**(2), 147-158 (2013).

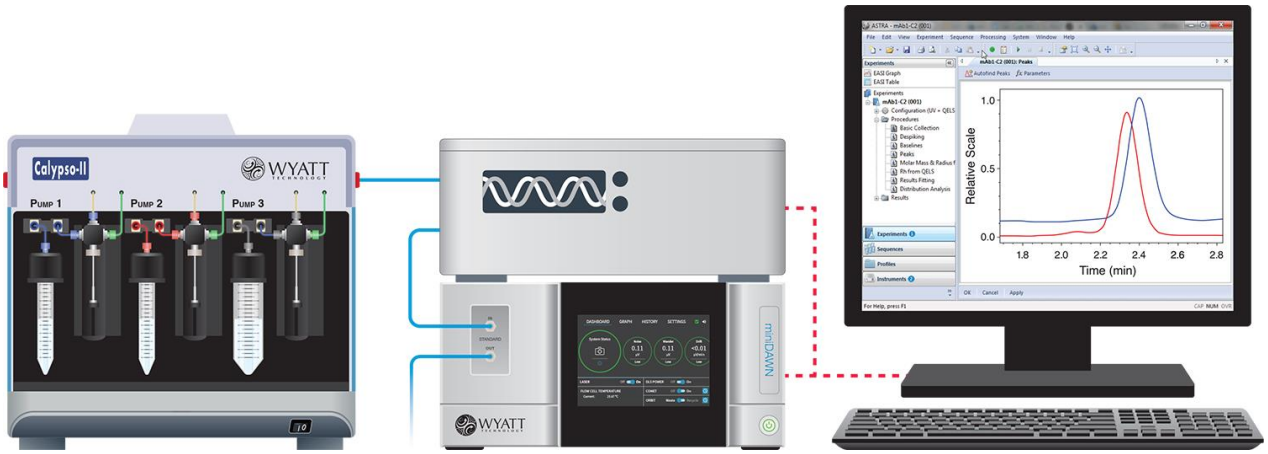

WHITE PAPER

WP5004: The diffusion interaction parameter (k_D) as an indicator of colloidal and thermal stability

Sophia Kenrick, Ph.D. and Daniel Some, Ph.D., Wyatt Technology Corp.

Summary

Stability is a key quality attribute in formulation studies of potential therapeutic biomolecules. In order to minimize time, effort and funds spent on stability studies, researchers rely on high-throughput screening methods that can reliably test hundreds of combinations of candidates, excipients and buffer conditions. Techniques utilized in these screens must determine a variety of stability-indicating parameters (SIPs). Some of the most useful SIPs to date are short term aggregation, thermal stability, and colloidal stability.

The ability to screen protein formulations at the early stages of development enables scientists to concentrate on the most suitable candidates, therefore saving substantial amounts of time, sample and testing equipment. This experiment demonstrates that thermal and colloidal stability of proteins, two indicators of propensity to aggregate, as well as actual aggregation states, are all determined simultaneously during the screening process with dynamic light scattering (DLS) tools in order to rank the effectiveness of candidates and formulation conditions. DLS can also indicate chemical stability and the average molar mass and specific volume of molecules in solution. For these reasons, HTS-DLS provides substantial quantities of information for the rapid screening of candidate molecules, buffer conditions and excipients, allowing the DynaPro® Plate Reader to maximize productivity in formulation studies.

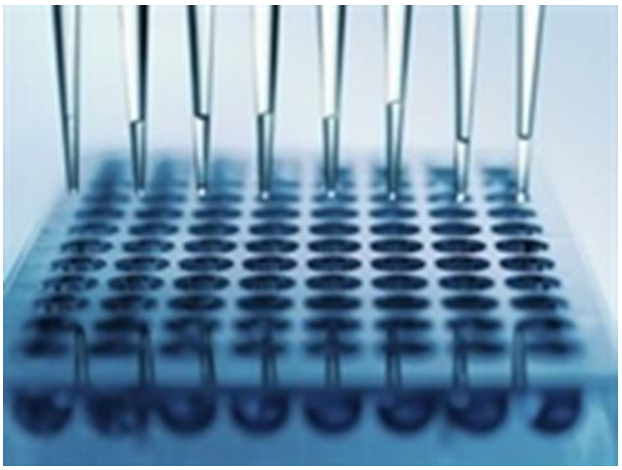

The DynaPro Plate Reader enables reliable testing of thousands of combinations of candidate biotherapeutics, excipients and buffer conditions in formulation studies.

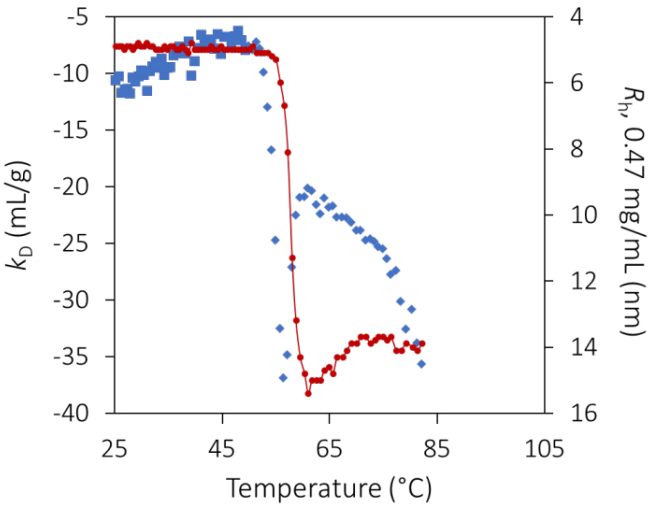

The diffusion interaction parameter k_D, measured by dynamic light scattering, identifies the onset of protein unfolding and its impact on colloidal stability, before indications apparent in the hydrodynamic radius

Introduction

Stability is a key quality attribute of therapeutic biomolecules, critical for establishing drug-like properties and suitability for use in humans. However, establishing the stability of a candidate molecule or formulation can be a long and tedious process. In order to minimize time, effort and funds spent on long-term stability studies, developers of biologics look to high-throughput screening methods that can reliably test and rank hundreds of combinations of candidates, excipients and buffer conditions. Experimental techniques utilized in these screens must determine a variety of stability-indicating parameters (SIPs), since no one parameter has yet proven to be the silver bullet indicative of long-term shelf life or stability under a variety of environmental stresses such as freeze-thaw or elevated temperatures.

Some of the most useful SIPs to date are: short term aggregation (the formation of, usually, small aggregates); thermal stability (the tendency of a protein to unfold and/or aggregate with temperature, usually as a consequence of exposure of the hydrophobic core); and colloidal stability (the tendency of molecules to associate due to weak, attractive forces related to surface charges, hydrophobic surface residues and similar moieties). These SIPs are not entirely independent of each other. For example, even though colloidal stability generally pertains to reversible association, the enhanced proximity under self-attractive conditions can enhance irreversible aggregation rates. Conversely, increased surface charge may reduce colloidal attraction and improve colloidal stability, yet degrade thermal stability as the charges destabilize the protein's tertiary structure.

A variety of techniques such as differential scanning calorimetry, intrinsic and extrinsic fluorescence, circular dichroism, infrared or Raman spectroscopy and static light scattering have been applied to assess SIPs. One technique in particular stands out for its great versatility: dynamic light scattering (DLS). DLS provides quantitative insight into a broad range of phenomena related to stability, as it can *simultaneously* quantify aggregation and distribution of aggregate sizes; thermal stability, discriminating between pure unfolding and aggregation through a temperature transition; and colloidal stability, via the concentration dependence of diffusion. The same instrument can also determine, at the same time, average molar mass and specific volume via static light scattering (SLS).

The stability of a biomolecule is not a wholly intrinsic property, but depends on buffer composition and the concentration at which the protein is formulated. Protein stability must be quantified as a function of pH, ionic strength, specific ion type and excipient profile for an optimal and successful formulation. Fortunately, DLS and SLS are amenable to high-throughput, low-volume screening of hundreds of conditions per hour by means of a plate reader utilizing industry-standard microwell plates. High-throughput screening by dynamic and static light scattering (HTS-DLS/SLS) is accomplished by means of the DynaPro Plate Reader which accommodates 96, 384 or 1536-well plates, performing temperature scans of all samples *in parallel* from 4 °C – 85 °C. The multiplexed approach provided by HTS-DLS/SLS can be extended to a variety of other formulation conditions for rapid characterization of protein behavior.

The *simultaneous* measurement of thermal and colloidal stability offers qualitatively novel information: the direct interaction between thermal and colloidal stability mechanisms, reflected in the temperature dependence of the colloidal interaction parameter in the vicinity of a thermal transition. This article demonstrates HTS-DLS measurements revealing the impact of thermally-induced protein unfolding on colloidal interactions, yet another quantitative metric for rapid ranking of protein formulations.

The Interaction Parameter

DLS directly measures fluctuations in scattering intensity due to Brownian motion, which are analyzed to determine the translational diffusion coefficient D_t and hence an effective measure of molecular size, the hydrodynamic radius R_h. DLS can also provide a rough measure of size distributions in order to assess populations of monomers and aggregates[1]. Though not as rigorous as a separation technique such as size exclusion chromatography coupled to light scattering detectors (SEC-MALS), this is often sufficient for screening purposes and will even indicate the presence of size populations that differ by 3- 5x in radius.

As a consequence of non-specific protein-protein interactions arising primarily from charged and hydrophobic residues, D_t is a function of concentration, c. Analysis of D_t vs. c leads to the first-order diffusion interaction

parameter k_D (not to be confused with the equilibrium dissociation constant K_d), per equation 1:

$$D = D_0 (1 + k_D c + \ldots) \quad \text{Eq. 1}$$

Positive values for k_D are indicative of repulsive intermolecular interactions while negative values indicate attraction.

The diffusion interaction parameter is directly related to the second virial coefficient A_2, a commonly-accepted thermodynamic measure of colloidal stability and propensity for aggregation[2,3]. Initial theoretical work put the relationship between k_D, A_2, the specific volume v and the first-order concentration coefficient of friction ζ_1 as Eq. 2a, or with some additional refinement as Eq. 2b[4].

$$k_D = 2A_2M - v - \zeta_1 \quad \text{Eq. 2a}$$

$$k_D = 2A_2M - 2v - \zeta_1 \quad \text{Eq. 2b}$$

Recently a detailed analysis of the various thermodynamic and hydrodynamic contributions to k_D for monoclonal antibodies resulted in a more precise relationship that agrees remarkably well with empirical results[5], stated in Eq. 3.

$$k_D = 1.024 \cdot A_2M - 6.18 \quad \text{Eq. 3}$$

As a result, k_D can be utilized to rapidly compare different protein formulations and guide the selection or engineering of more stable biomolecules[6–11].

Materials and Methods

A DynaPro Plate Reader ran HTS-DLS measurements for simultaneous thermal, colloidal and mixed stability analyses, also assessing the degree and size distribution of aggregation. A significant benefit of this instrument is measuring the sample directly in the well, eliminating concerns of carry-over common to microfluidic platforms, while boosting throughput.

A monoclonal antibody (mAb1) was dissolved in 50 mM bis-tris-propane buffer (BTP) at pH values of 6.5, 7.5, 8.5 and 9.5 to a final concentration of 15 mg/mL. This stock solution was filtered to 0.1 µm and then diluted and arrayed in a 384-well microtiter plate (Aurora) at five replicates of six different protein concentrations between 0.47 mg/mL and 15 mg/mL, for each of the four pH values, loading 20 µL of solution into each well. The plate was centrifuged at 400 x *g* for 1 minute and each well was then capped with 1-2 drops of paraffin oil to prevent evaporation. Prior to measurement, the plate was centrifuged again at 400 x *g* for 1 minute.

Initial measurements at 25 °C included control samples of bovine serum albumin and lysozyme in the same plate, not discussed here (though the measurements appear in some figures). An extended series of measurements was then conducted as a function of temperature, ramping from 25 °C to 85 °C at a rate of 0.1 °C/min. During the ramp the mAb1 solutions were measured sequentially, completing five 2-second acquisitions for three replicate wells at each concentration and pH, every 0.5 °C.

Instrument control, data acquisition and analysis were carried out via the DYNAMICS software and Microsoft Excel. D_t and R_h were determined from autocorrelation analysis and k_D was calculated from the linear regression of D_t vs. c. Aggregation onset temperature T_{onset} was determined per concentration and pH by fitting the plot of R_h vs. temperature to an appropriate model.

Results and Discussion

Interaction parameter as a function of pH

MAb1 exhibited increasing R_h (decreasing D_t) as a function of concentration (Figure 1), corresponding to a negative k_D and hence protein-protein attraction. This antibody exhibits $k_D < 0$ for all pH values tested (Figure 2), indicating a predisposition to assemble into oligomeric species.

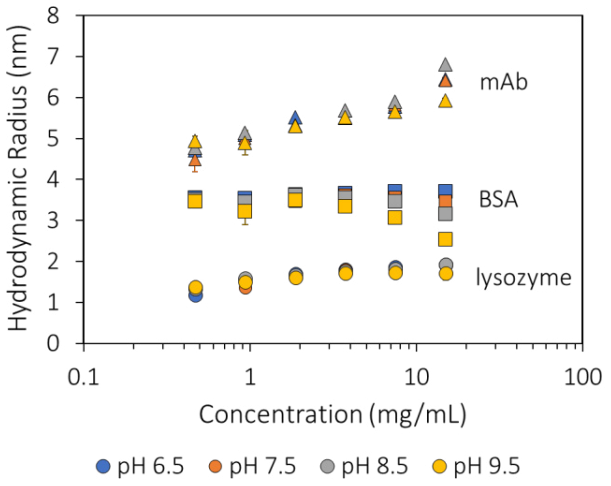

Figure 1: Measured hydrodynamic radius as a function of concentration and pH for three proteins.

Thermally induced aggregation

At pH 8.5 mAb1 rapidly aggregates into large complexes beyond the thermal transition around 55 °C, with R_h at 75 °C ranging from 80 nm to 800 nm (Figure 3). T_{onset} decreases with concentration, ranging from 55.0 to 56.8 °C (Figure 3, inset). The final aggregation state is highly dependent on the concentration, varying by over two orders of magnitude in average particle size between the lowest and highest concentrations.

A second transition occurs at 70-75 °C, possibly related to the unfolding of another IgG domain, that results in large-scale aggregation into particles >1 µm. The high degree of aggregation suggests that the observed concentration dependence past the thermal transition is primarily a consequence of higher molecular collision rates. This can be confirmed by varying the temperature ramp rate.

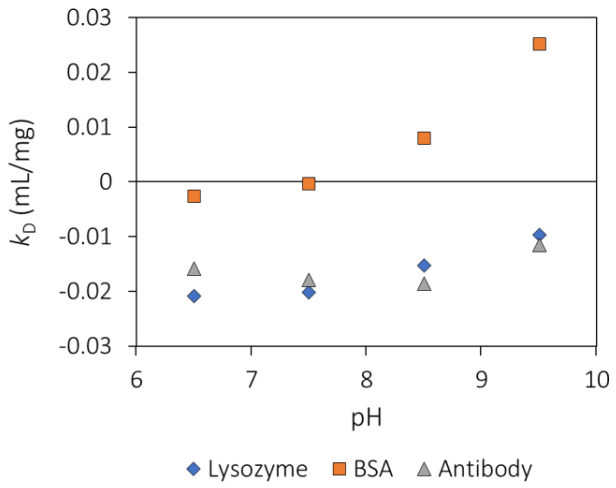

Figure 2: Interaction parameter, k_D, as a function of pH for three proteins.

In contrast, at pH 9.5, mAb1 exhibits a shift from a typical IgG monomer size of R_h = ~4.8 nm to a stable value between 15 and 22 nm, depending on concentration, for temperatures above 62 °C (Figure 4). The small size and high stability of the aggregates at this pH suggest reversible oligomerization. This can be confirmed by reversing the temperature ramp and/or varying the ramp rate.

Around 75 °C, the antibody appears to enter a second unfolding transition, similar to pH 8.5 though with much smaller magnitude of aggregation and little effect at the lower concentrations.

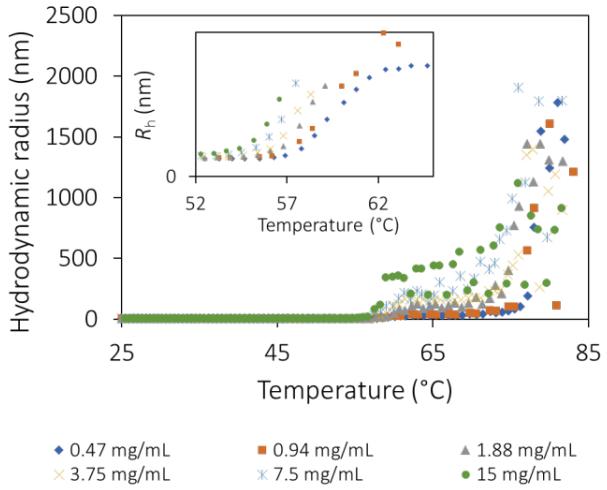

Figure 3: Hydrodynamic radius as a function of temperature and concentration for an antibody formulation at pH 8.5. High order aggregate formation is evident for temperatures > 56 °C.

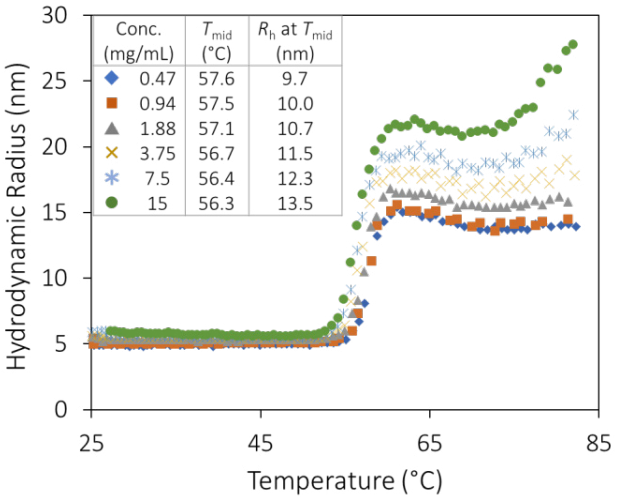

Figure 4: The hydrodynamic radius exhibits a sigmoid relation-ship as a function of temperature for all antibody concentrations at pH 9.5, showing little change in the midpoint with con-centration.

The qualitative difference in aggregation processes the two conditions are further elucidated in the size distributions obtained with DLS regularization analysis. At 80 °C, the pH 8.5 sample with 1.88 mg/mL concentration exhibits a bimodal distribution with populations around 30- 100 nm and 300- 3000 nm, while the pH 9.5 sample at the same concentration presents a single distribution at 80- 300 nm, as shown in Figure 5.

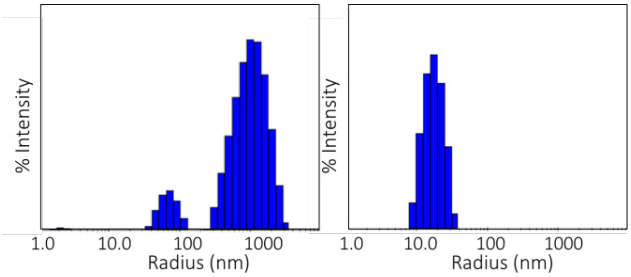

Figure 5: Size distributions obtained at 80 °C via regularization. Left: pH 8.5; right: pH 9.5.

Interaction parameter through the thermal transition

Below the thermal transition, k_D is negative and approximately constant with temperature increase for both pH values. The magnitude of k_D at pH 8.5 is about twice that of pH 9.5, indicating stronger intermolecular attraction, which correlates to the vastly different aggregation behavior. In the vicinity of the folding-unfolding transition and onset of aggregation, k_D exhibits distinct transition behavior versus pH.

At pH 8.5, k_D undergoes a dramatic step-change from between 53 °C and 59 °C (Figure 6 and inset). Strikingly, the shift begins several degrees before any appreciable aggregation appears and is suggestive of increased protein-protein attraction due to pure unfolding. Beyond 59 °C, k_D is constant (though noisy due to the numerical difficulty of ascribing a single average radius when the population is bimodal). As seen in Figure 3, the degree of aggregation depends on concentration, but this would appear to be due primarily to higher collision rates and therefore the measured value of k_D beyond ~ 56 °C probably is not indicative of a true thermodynamic interaction, but rather of the history and kinetics of the aggregation process.

A similar change in k_D signals the unfolding transition at pH 9.5: once again k_D becomes more negative (more attractive) several degrees prior to aggregation. Instead of a step-change, however, we now observe a local *minimum* occurring just as the measured hydrodynamic radius begins to indicate aggregation (Figure 7). Upon aggregation, the magnitude of k_D decreases to become less negative. This trend in k_D indicates once more that attractive interactions increased during the first unfolding transition as the hydrophobic core is exposed. However, in this condition, once a stable structure has been achieved, these interactions are partially mitigated as the exposed regions are now hidden from the solution.

A secondary unfolding transition around 75 °C is clearly reflected in k_D.

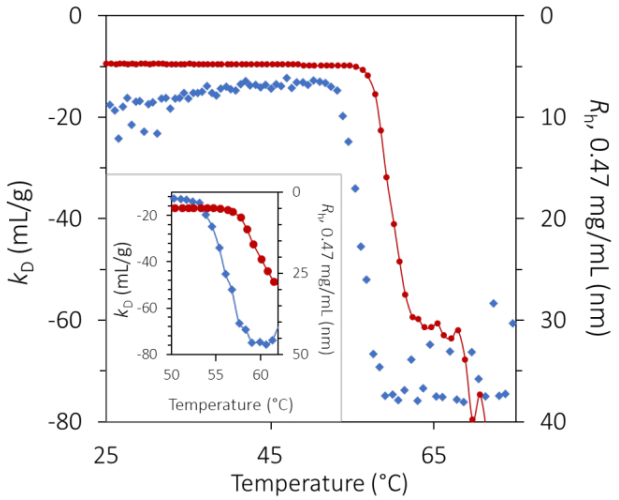

Figure 6: Diffusion interaction parameter (blue diamonds, left axis) and radius (red circles and solid line, right inverted axis) at lowest concentration as a function of temperature at pH 8.5. Inset: same, highlighting the transition region.

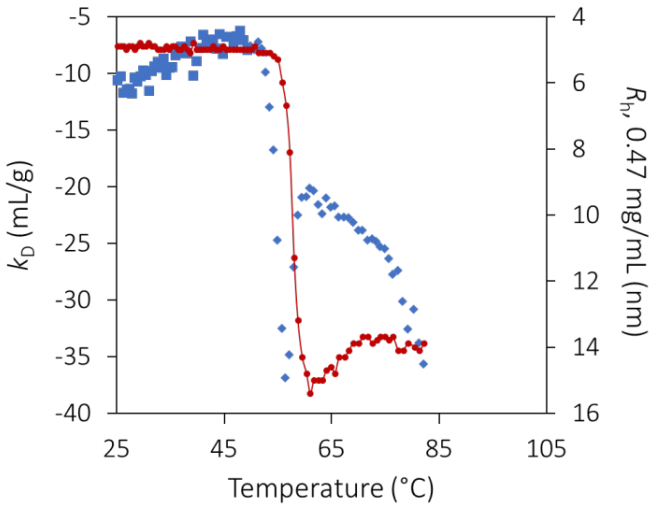

Figure 7: Diffusion interaction parameter (blue diamonds, left axis) and radius (red circles and solid line, right inverted axis) at lowest concentration as a function of temperature at pH 9.5. Inset: same, highlighting the transition region.

Conclusions

The ability to screen protein formulations at the early stages of development enables scientists to concentrate on the most suitable candidates and so save substantial amounts of time, sample and testing equipment. This experiment demonstrates that thermal and colloidal stability of proteins, two indicators of propensity to aggregate, as well as actual aggregation states, are all determined simultaneously during the screening process with the DynaPro Plate Reader III in order to rank the effectiveness of candidates and formulation conditions.

Thermal stability is quantified as T_{onset} and colloidal stability as k_D. The temperature dependence of k_D provides unique insight into the effect of unfolding on colloidal interactions, as the unfolding process reveals moieties previously 'hidden' from buffer and other proteins. Not discussed here, DLS can also indicate chemical stability and the average molar mass and specific volume of molecules in solution as a function of temperature, as well as solution viscosity[12] which is another important factor in formulating high-concentration biotherapeutics. Therefore, HTS-DLS provides substantial quantities of information for the rapid screening of candidate molecules, buffer conditions and excipients in order to drive higher productivity.

References

1. Jocks, T. & Roessner, D. Performing Automated Dynamic Light Scattering Using Plate Reader Technology. *Int. Pharm. Ind.* **2**, 22–25 (2009).
2. Some, D. & Hitchner, E. Characterizing protein-protein interactions via static light scattering: Nonspecific interactions. *ResearchGate* https://www.researchgate.net/publication/291838630_Characterizing_protein-protein_interactions_via_static_light_scattering_Nonspecific_interactions.
3. Kuehner, D. E. *et al.* Interactions of lysozyme in concentrated electrolyte solutions from dynamic light-scattering measurements. *Biophys. J.* **73**, 3211–3224 (1997).
4. Teraoka, I. Polymer Solutions: An Introduction to Physical Properties | Wiley. *Wiley.com* https://www.wiley.com/en-ly/Polymer+Solutions%3A+An+Introduction+to+Physical+Properties-p-9780471389293.
5. Roberts, D. *et al.* The Role of Electrostatics in Protein–Protein Interactions of a Monoclonal Antibody. *Mol. Pharm.* **11**, 2475–2489 (2014).
6. He, F., Woods, C. E., Becker, G. W., Narhi, L. O. & Razinkov, V. I. High-throughput assessment of thermal and colloidal stability parameters for monoclonal antibody formulations. *J. Pharm. Sci.* **100**, 5126–5141 (2011).
7. Lehermayr, C., Mahler, H.-C., Mäder, K. & Fischer, S. Assessment of net charge and protein-protein interactions of different monoclonal antibodies. *J. Pharm. Sci.* **100**, 2551–2562 (2011).
8. Saito, S. *et al.* Effects of ionic strength and sugars on the aggregation propensity of monoclonal antibodies: influence of colloidal and conformational stabilities. *Pharm. Res.* **30**, 1263–1280 (2013).
9. Menzen, T. & Friess, W. Temperature-Ramped Studies on the Aggregation, Unfolding, and Interaction of a Therapeutic Monoclonal Antibody. *J. Pharm. Sci.* **103**, 445–455 (2014).
10. Zidar, M., Šušterič, A., Ravnik, M. & Kuzman, D. High Throughput Prediction Approach for Monoclonal Antibody Aggregation at High Concentration. *Pharm. Res.* **34**, 1831–1839 (2017).
11. Esfandiary, R., Parupudi, A., Casas-Finet, J., Gadre, D. & Sathish, H. Mechanism of reversible self-association of a monoclonal antibody: role of electrostatic and hydrophobic interactions. *J. Pharm. Sci.* **104**, 577–586 (2015).
12. He, F. *et al.* High-throughput dynamic light scattering method for measuring viscosity of concentrated protein solutions. *Anal. Biochem.* **399**, 141–143 (2010).

WYATT TECHNOLOGY

WHITE PAPER

WP5010: Screening Developability and Pre-Formulation of Biotherapeutics with High-Throughput Dynamic Light Scattering (HT–DLS)

Daniel Some, Ph.D., Wyatt Technology Corp.

Introduction

Assessing a drug candidate's suitability early in the discovery and development stages is essential for minimizing the risk of costly downstream failure. Multiple aspects of a biotherapeutic molecule's behavior and suitability as a drug candidate may be quantified via biophysical analysis techniques:

- **functionality** (binding to targets/antigens and effectors)
- **homogeneity/purity** (the presence of aggregates or fragments)
- **stability** (the tendency to degrade via changes in higher-order structure as well as chemical modifications).

Viscosity of a concentrated protein solution is another important performance parameter amenable to biophysical analysis; formulations with high viscosity are not suitable for manufacturing or intravenous delivery.

One of the primary technologies for assessing aggregation, stability and viscosity of biotherapeutics, from proteins and peptides to attenuated viruses, is dynamic light scattering (DLS).[1] DLS measures particle size and size distributions, from less than a nanometer and up to several microns, without perturbing the sample. The measurement takes place on time scales of seconds to minutes, and the sample is fully recoverable. This makes DLS a particularly effective technique for assessing aggregation and stability in early as well as late stages. In addition, viscosity can be measured via DLS using probe particles such as common polystyrene latex beads.

HT-DLS maximizes productivity

Traditional DLS measurements take place manually, one at a time, in cuvettes, resulting in low throughput and low productivity. Cuvette-based analysis limits the number of candidates and formulations that can be analyzed, restricting the implementation of highly efficient development strategies such as quality by design (QbD) and Design of Experiments (DoE).

Automated, high-throughput dynamic light scattering (HT–DLS) utilizing Wyatt Technology's DynaPro® Plate Reader (DPR) helps streamline the candidate selection and pre-formulation processes. HT-DLS provides more data, on more samples and more formulations—typically *10x – 100x more measurements* than would be collected using cuvette-based DLS, but with far less effort.
The DPR can be used as a standalone instrument or as part of a larger automated formulation workflow[2]. Using just a few microliters of solution per sample in standard microwell plates, unattended HT–DLS measures multiple biotherapeutic candidates in a variety of formulation and environmental conditions.

Dynamic light scattering instrumentation

Dynamic light scattering (DLS) uses a sensitive detector to monitor the intensity fluctuation of scattered light that arises from the Brownian motion of particles in solution. DYNAMICS software then analyzes the autocorrelation data to determine the rate of diffusion, which is converted to hydrodynamic radius via the Stokes-Einstein equation, $R_h = k_B T / 6\pi\eta D_t$.

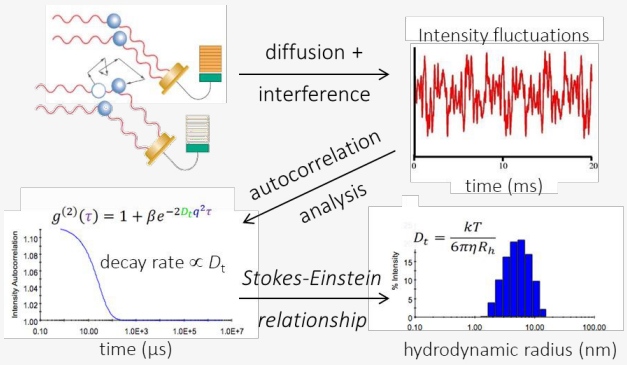

The Stokes-Einstein equation relates light scattering intensity and Brownian motion to hydrodynamic radius.

The DynaPro Plate Reader carries out high-throughput DLS measurements of the size and interactions of proteins, nanoparticles, and other macromolecules. The instrument automatically self-adjusts its sensitivity by a factor of up to 10^5 in order to accommodate a wide range of particles sizes and concentrations.

In addition to DLS, the DPR measures static light scattering (SLS) which enables determination of the weight-average molar mass M_w of a solution, which can confirm aggregation. SLS also measures non-specific protein-protein interactions via the second virial coefficient, A_2.

Since the DLS and SLS measurements are completed *in situ* in industry-standard microwell plates, liquid handling is minimized. This capability reduces measurement time and eliminates sample carryover, resulting in a typical scan time of less than one hour for a 96 well plate. Users can also program customized temperature ramps in order to assess thermal behavior, and test protein properties such as the onset temperature and the rate of unfolding or aggregation.

HT-DLS provides rapid, comprehensive studies, resulting in greater confidence in the final selection of candidate or formulation. With the advent of 21CFR11-compliant software for the DPR, DYNAMICS® SP, this instrument is suitable for all GLP and GMP labs that need to determine the size, stability and viscosity of biotherapeutics.

This white paper introduces the technology that powers automated HT–DLS and explores its practical applications in candidate and formulation selection.

HT-DLS for Developability and Pre-formulation Studies

DLS is a non-invasive, non-perturbative method of measuring protein and particle size distribution in terms of hydrodynamic radius (R_h) across a wide range, covering 0.2 – 2500 nm in cuvette-based instruments and 0.5 – 1000 nm in HT-DLS. The fundamental strength of DLS is its ability to determine changes in protein size, conformation and aggregation/oligomerization state across a range of conditions, allowing users to rigorously investigate a candidate's behavioral profile.

The measurement of DLS does not depend on ambiguous reporter signals like intrinsic or extrinsic fluorescence, or exothermic or endothermic processes, all of which may fail to indicate those conformational changes of actual significance to stability. Rather, DLS directly indicates a true physical change in conformation as well as aggregation state.

DLS delivers essential insight into biopharmaceutical candidates and formulations, including

- Aggregation of nanometer to submicron particulates
  - ✓ before and after applied stress
  - ✓ during accelerated thermal stress
  - ✓ under pH stress
- Stability and aggregation propensity studies
  - ✓ colloidal stability/self-association, via concentration dependence
  - ✓ thermal conformational stability, via temperature ramps
  - ✓ chemical denaturation conformational stability, via denaturant gradients
- Viscosity of high-concentration protein formulations.

Traditional manual, cuvette-based DLS is suitable for testing a handful of samples, but not hundreds. Automation helps to resolve the challenge of analyzing hundreds of samples and conditions; HT-DLS experiments improve statistics, allow for multiple replicates, and are completed in a fraction of the time of manual analyses. With data generated as rapidly as 10 seconds per well, an experiment covering 384 sample wells consisting of a variety of different candidates, pH values, ionic strengths and replicates can be completed in just 90 minutes.

The DPR employs industry-standard well plates compatible with other plate-based screening techniques. In practice, this means DLS samples are easily transferable to other instruments for multivariate sample analysis. The ability to rapidly scope a drug product's performance under hundreds of different conditions allows scientists to more readily implement DoE and QbD methods, in order to meet regulatory and corporate productivity expectations.

The following examples illustrate the effective application of automated HT–DLS for a number of essential aggregation and stability investigations.

Measuring gross aggregation

Protein aggregation is a major concern during biopharmaceutical development. Unchecked aggregation reduces the efficacy of a biotherapeutic, affects its manufacturability, and may present a serious immunogenic risk.

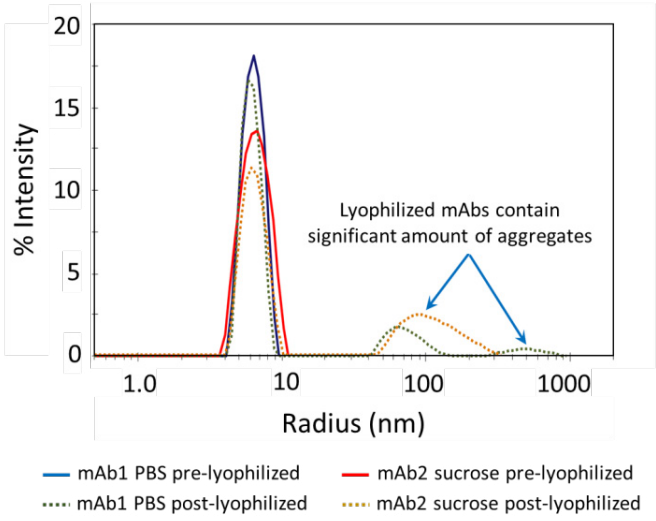

Figure 1: HT–DLS quantifies gross aggregation. Following lyophilization and reconstitution, a monoclonal antibody (mAb) solution containing PBS is shown to aggregate in the submicron size region.

By monitoring changes in particle size distribution with DLS, formulators are able to map out protein aggregation as a function of pH or excipient concentration. Alternatively, aggregation may be tracked through a dynamic temperature range, or followed during key waypoints in the formulation process. For example, Figure 1 shows the particle size distribution of two monoclonal antibody (mAb) formulations with and without sucrose, before and after lyophilization, measured using the DPR. Lyophilized samples were reconstituted to the same concentration as pre-lyophilized solutions.

Before lyophilization, the size distributions of both samples were monomodal. The pre-lyophilized solution containing sucrose (Figure 1, solid red line) has a marginally wider distribution peak, which suggests that the small sucrose molecules impart some polydispersity. It is clear that the lyophilized mAbs contain large aggregates, with the PBS sample in particular forming extremely large species post-lyophilization (Figure 1, green dotted line).

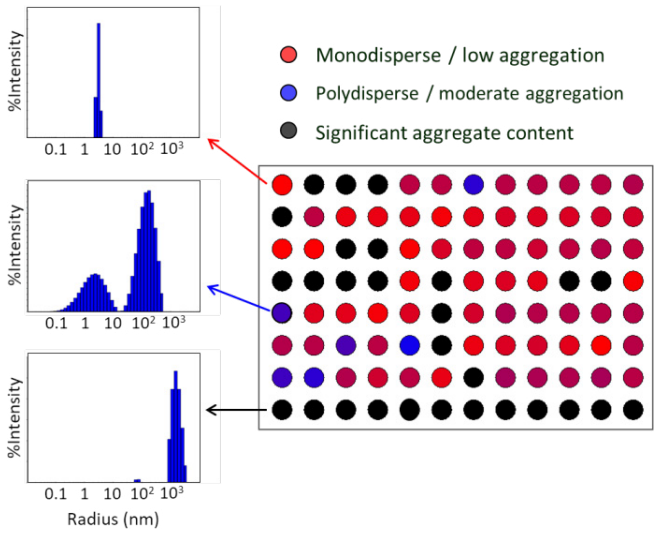

Figure 2: The heat map display in DYNAMICS may be programmed to differentiate size distributions and visualize at a glance different degrees of aggregation. Data courtesy Sabin Vaccine Institute.

Despite the intensity of the post-lyophilized aggregate peaks between 50-200 nm, the number of these aggregates is actually very small. Converting these data to percent mass via DYNAMICS software reveals that although the lyophilized antibody's primary peak between 4-10 nm has an integrated intensity of only 80%, its total percentage mass was 99.6%. Aggregates in the 50-200 nm range, therefore, account for only 0.4% of the overall protein population. Whether this percentage falls

within the limits of suitability depends on the candidate; the role of HT–DLS is to quickly provide the information required for formulators to make this decision.

Rapid visualization of the aggregation behavior of dozens or hundreds of samples in a plate is accomplished via heat maps such as the one shown in Figure 2. Color coding was applied to differentiate between unaggregated, lightly aggregated and heavily aggregated samples (red, blue and black, respectively). This visualization approach allows users to quickly obtain an overview of the results and pick out regions of the plate corresponding to specific excipients, pH conditions or candidate molecules that appear promising for further study.

Imaging contaminants and precipitates

The DPR is equipped with a camera that can be programmed to acquire images of each well after DLS measurement. One of the benefits of the camera is the ability to discern precipitation, since particulates sink to the bottom of the well, as shown in Figure 3.

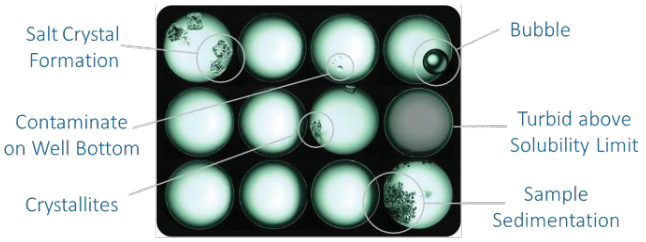

Figure 3: Tiled images from the DynaPro Plate Reader's onboard camera. Left: wells containing no precipitates or other contaminants. Right: wells containing a variety of contaminants.

Measuring thermal conformational stability

DLS allows formulators to probe other aspects of protein behavior, such as conformational changes across a dynamic temperature range. Figure 4 shows a temperature scan of lysozyme in an acetate buffer of pH 4. Lysozyme proteins fold and unfold readily without aggregation. In this case, the molecular size of the sample began increasing around 65°C before reaching a plateau around 90°C. T_m indicates the midpoint for the transition. When the transition does not allow for setting a midpoint, T_{onset} is used to indicate the onset temperature.

When lysozyme was held at 90°C for multiple readings, the size remained constant, indicating unfolding but not aggregation. This behavior is typical of single-domain proteins but not of multi-domain proteins.

Moreover, the DPR incorporates static light scattering (SLS) measurements, enabling users to differentiate between folding and aggregation behavior. SLS is calibrated to provide molar mass (assuming the protein concentration is known), a property that increases in value during aggregation but remains unchanged during purely conformational changes. In the case of lysozyme, the change in size is not accompanied by a change in SLS (not shown), supporting the conclusion that the protein is unfolding rather than aggregating.

Instruments that measure intrinsic fluorescence and SLS simultaneously utilize short-wavelength illumination to assess aggregation. However, UV is known to actually induce protein aggregation[3], making this approach to aggregation analysis highly suspect. The wavelength of the DynaPro Plate Reader, 830 nm, is not capable of inducing aggregation, guaranteeing a reliable measurement.

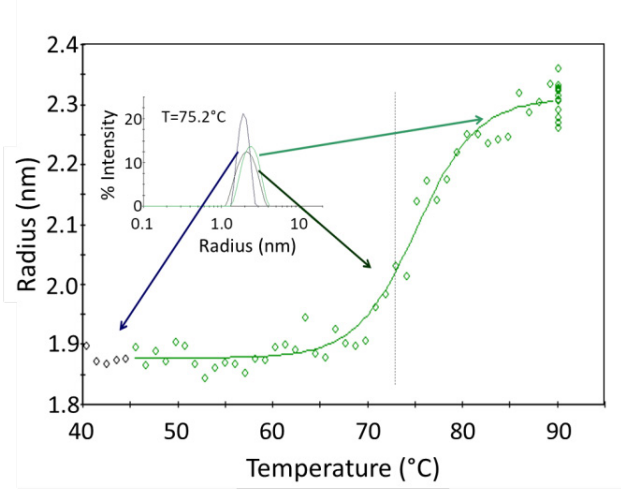

Figure 4: Dynamic light scattering (DLS) is used to measure conformational changes in structure, such as the unfolding of lysozyme across a dynamic temperature range.

A multi-domain protein, IgG, exhibits both unfolding and aggregation as shown in Figure 5. While the large changes in both size (DLS) and count rate (uncalibrated SLS) above 60 °C are clearly associated with aggregation, a closer look in the vicinity of the transition temperature clarifies the different onset temperatures for unfolding (58 °C) and aggregation (59 °C). The temperature ramp rate was relatively slow at 0.1 °C/min, so the temperature lag is probably not a kinetic effect associated with the time lag.

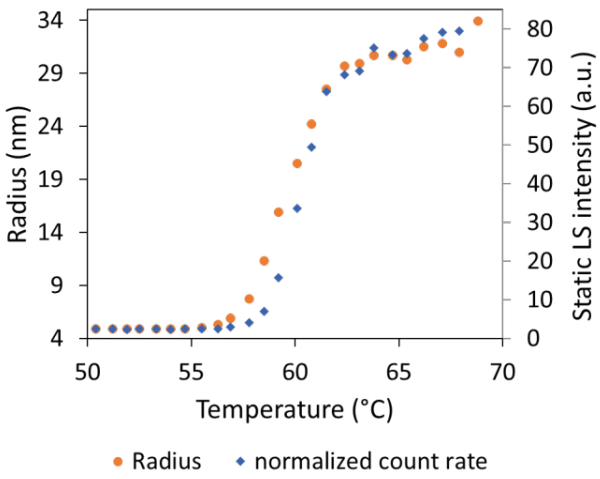

Figure 5: Unfolding vs. aggregation in 0.47 mg/mL monoclonal IgG, identified by DLS and SLS (i.e., the DLS count rate). Unfolding is seen to precede aggregation by about 1 °C, exhibited in the delayed onset of SLS intensity increase relative to the increase in radius.

Holding a series of formulations at a constant temperature and measuring the rate of aggregation as expressed in the changes in particle size (radius) and molecular weight is another effective way to assess stability and rank-order formulations. This type of stability assay should generally be performed at a temperature well below the temperature of unfolding. HT-DLS affords parallel aggregation-rate measurements of large numbers of candidates and/or formulation conditions.

Utilizing both temperature ramps and accelerated aggregation at a fixed temperature, the DPR provides invaluable insight into the nature of protein interactions in solution and the transition temperature at which conformational changes give way to aggregation.

Measuring chemical conformational stability

An additional means for quantifying a molecule's stability against conformational changes is chemical denaturation gradients. A denaturant such as urea or guanidine HCl is titrated into the protein solution in order to determine the denaturant concentration at which the molecule is present in equal amounts as folded and unfolded species, and hence the Gibbs free energy of unfolding.

The common method for assessing unfolding in a chemical denaturation measurement is intrinsic fluorescence. However, DLS is a superior quantifier of unfolding since it does not rely on the presence of fluorophores, does not lead to photon-induced damage, and is a positive, reliable indicator of unfolding via changes in actual size. Chemical denaturation screening of a multi-domain protein was demonstrated in the DynaPro Plate Reader by Yu *et al.*[4]

HT-DLS offers key advantages over other techniques used to study thermal and chemical conformational stability, such as intrinsic fluorescence or differential calorimetry:

- By directly reporting changes in size, there is no guesswork involved in determining whether the signal relates to a conformational change or is a spurious result of changes in the chemical environment.
- Unfolding without aggregation is directly discriminated from aggregation.
- The nature and size distribution of aggregates that may form, whether reversible or irreversible, is determined.
- Intrinsic fluorescence is excited by short-wavelength UV which is known to induce protein aggregation even without thermally-induced denaturation. This phenomenon is particularly pronounced in antibody-drug conjugates[3].

Measuring aggregation propensity

HT–DLS also measures aggregation propensity (colloidal stability), enabling users to better predict stability at early phases of analysis or to secure more in-depth information of protein behavior around unfolding and aggregation transition points.

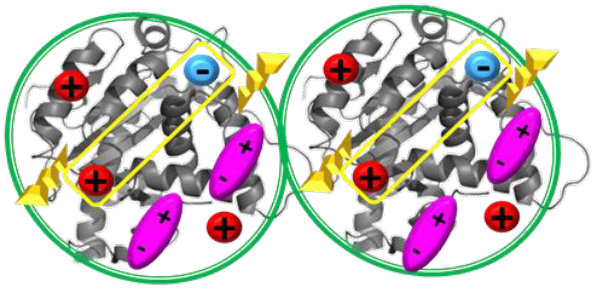

Figure 6: Colloidal instability is a result of the combined effects of surface charge distributions, local dipoles, hydrophobic patches, and other physical contributions to protein-protein interactions.

Colloidal stability analysis with DLS allows formulators to determine the magnitude of attraction between molecules in solution and is indicative of native-state protein-protein interactions such as those shown as a cartoon in Figure 6. This is accomplished by measuring the change in

a protein's diffusion coefficient as a function of concentration. If the diffusion coefficient decreases with a decrease in concentration, then larger particulates are forming and self-association occurs. If the coefficient increases with concentration, then molecules are likely repelling each other and are stable in solution.

These measurements are described by the diffusion interaction parameter k_D, the slope of the diffusion coefficient vs. concentration. The magnitude of k_D directly relates to aggregation propensity. When k_D is greater than 0, repulsive forces dominate and the solution is more likely to be stable. When k_D is less than 0, attractive forces dominate and the sample is likely to aggregate. The diffusion interaction parameter k_D has been shown to be an important stability-predicting parameter, perhaps even more useful to formulators than T_m[5].

Figure 7 shows the measurements of R_h as a function of concentration for three proteins in buffers with the indicated pH. The change in diffusion coefficient as a function of concentration, which is used to determine k_D, can also be viewed as a change in apparent hydrodynamic radius. A series of concentrations are prepared for each sample and each buffer condition, and these are loaded into microwell plates for DLS analysis. The set of 24 conditions per protein sample, each with 5 replicates, takes about 20-30 minutes to complete in the DPR. Figure 8 plots the k_D values vs. pH for each protein. Lysozyme and antibody are self-associative at all pH values, whereas BSA is stable above pH 7.

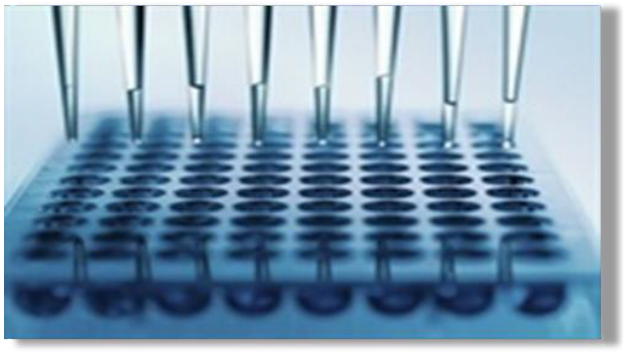

The DynaPro Plate Reader enables reliable testing of thousands of combinations of candidate biotherapeutics, excipients and buffer conditions in formulation studies.

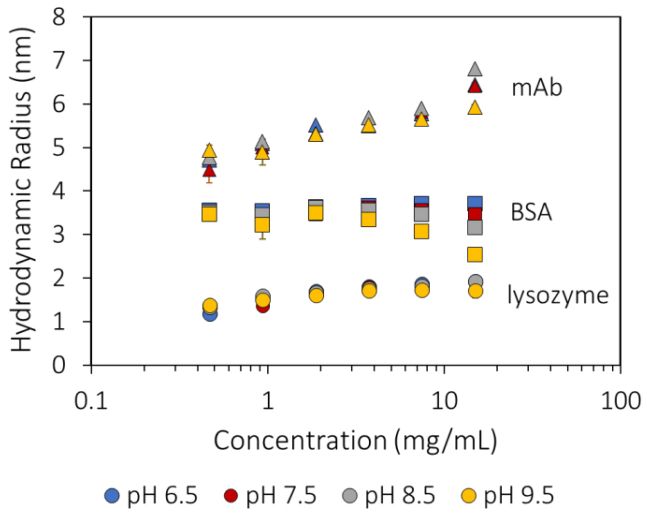

Figure 7: Measured hydrodynamic radius as a function of concentration and pH for three proteins, from which k_D may be determined.

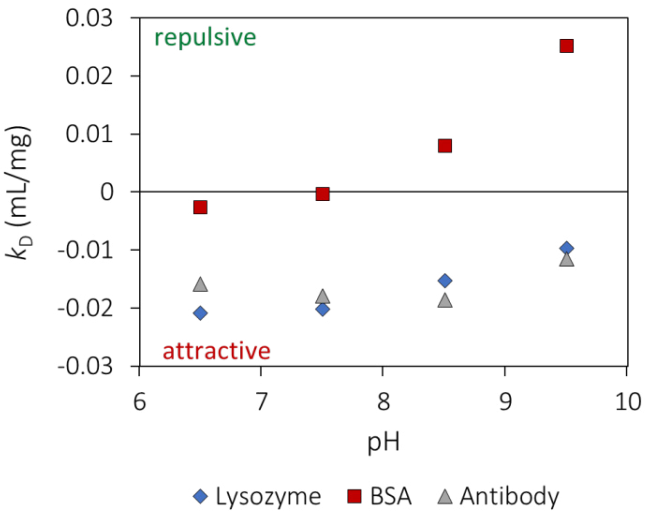

Figure 8: Interaction parameter k_D versus pH for three proteins.

As an indicator of protein-protein interactions, it can be especially informative to utilize k_D to understand the phenomena occurring upon unfolding. Figure 9 shows one example of how k_D changes with temperature around the unfolding transition of a mAb sample. At lower temperatures, k_D and R_h are fairly constant, approximately -10 mL/g and 5 nm, respectively. When the temperature exceeds 55°C, however, k_D increases significantly as aggregation begins. Several degrees before the point of aggregation, the value of k_D decreases sharply. This observation can be rationalized by considering the unfolding behavior of the protein around this point. As proteins unfold, their hydrophobic cores are exposed and the

molecules become self-attractive. The magnitude of k_D increases and the value becomes more negative at the onset of aggregation, indicative of the increase in attractive interactions. However, as aggregation progresses, the hydrophobic cores become hidden from the other molecules in solution and k_D again becomes less negative.

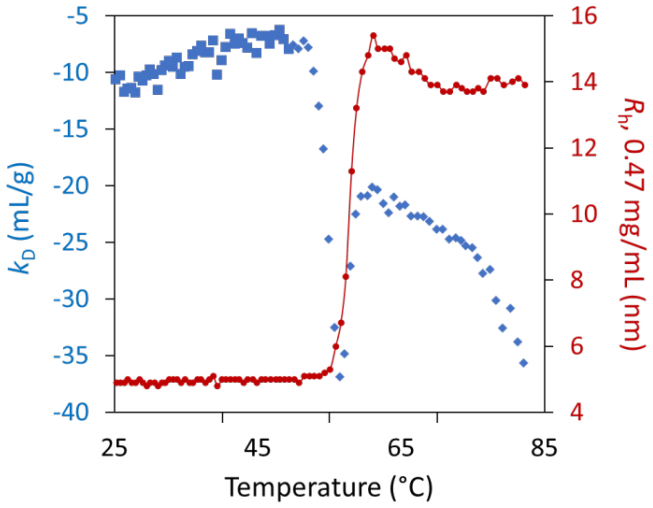

Figure 9: The diffusion interaction parameter, k_D, decreases prior to the point of aggregation as protein molecules begin to unfold.

A closer look at the vicinity of the transition region with the addition of SLS data (Figure 10) brings out three distinct transition temperatures: the onset of protein-protein interactions, at 52.2°C; the onset of unfolding, at 55.2°C; and the onset of aggregation at 57.3°C. The onset of interactions is most likely the result of a minor conformational change that creates intermolecular attraction but is insufficient to cause appreciable size increase.

One of the key advantages of DLS over other stability-indicating techniques is the ability to interrogate the types of aggregates that are formed, in addition to the degree of aggregation. Figure 11 presents the quite different aggregates created at high temperature under two different pH conditions.

While here only k_D is discussed, a closely related parameter is the second virial coefficient, A_2, which is determined simultaneously by means of SLS intensity versus concentration. While more challenging to measure than k_D, A_2 is a fully thermodynamic measure of colloidal stability and often considered of primary importance in assessing colloidal stability of proteins. Both may be determined simultaneously in the DynaPro Plate Reader.

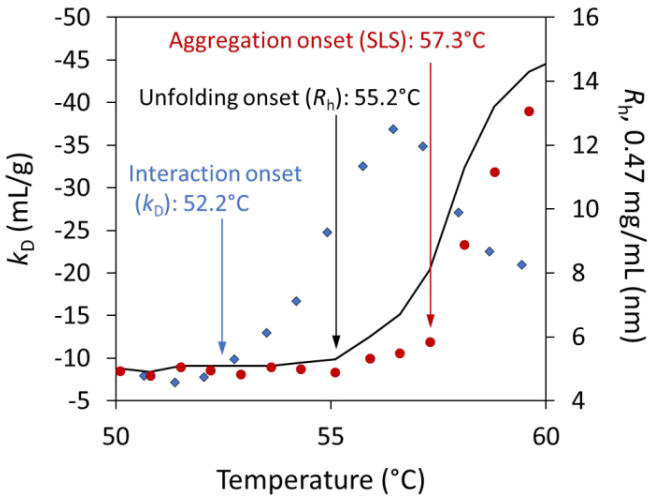

Figure 10 :The data of Figure 9, blown up in the vicinity of the thermal transition, with the addition of SLS data. Blue diamonds: k_D values; black line: R_h values; red circles: SLS values. Three distinct transition temperatures are evident. The k_D scale has been inverted for clarity.

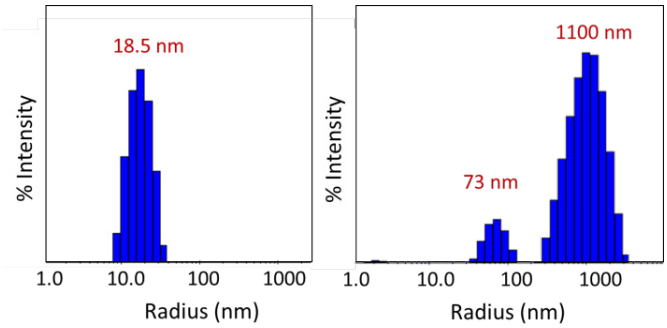

Figure 11: Size distributions obtained at 80°C via regularization. Left: pH 9.5, indicating aggregate species of ~ 18 nm; right: pH 8.5, indicating species with sizes of ~70 nm and ~ 1000 nm.

Using HT–DLS to determine viscosity

Finally, DLS can be used to assess formulation viscosity to help determine the long-term stability and deliverability of a biotherapeutic. DLS measures viscosity by spiking sample wells with polystyrene beads of a known diameter and radius, as shown in Figure 12. The Stokes-Einstein equation is manipulated to determine viscosity. The results from DLS have been shown to correspond well to traditional rheological techniques, such as ball-and-cone viscometry. The advantage of employing automated HT–DLS for viscosity measurements is that low-volume samples are assessed rapidly, in the same plates and at the same time as a variety of other features, adding a further layer of detail to scientists' understanding of their formulations.

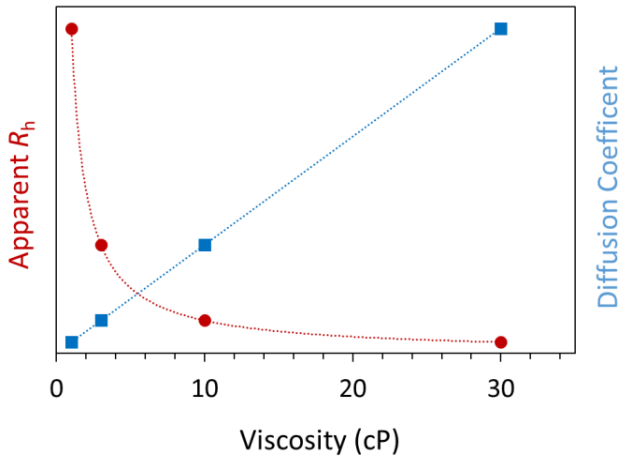

Figure 12: In DLS, increasing solution viscosity associated with higher protein concentration causes decreased diffusion and an apparent increase of radius of a probe particle of known size. The diffusion coefficient is analyzed to yield the solution viscosity.

Identifying the best candidates as early as possible

As the pharmaceutical industry targets increasingly complex biologic candidates, automated formulation and analytical workflows play an important role in streamlining the development process. Capable of performing 96 runs in under 45 minutes and 384 wells in 1.5 – 2 hours, with completely unattended operation, high performance HT–DLS accelerates analysis time, reduces the need for expert operator supervision, and improves confidence in data quality. This level of automation provides developers with the depth of data and resources necessary to implement highly efficient development strategies for better performing, safer biotherapeutics.

To learn more about HT-DLS, please visit www.wyatt.com/HT-DLS and www.wyatt.com/Webinars/DLS.

For more information on the DynaPro Plate Reader, see www.wyatt.com/DynaPro.

References

1. Rader, R. FDA Biopharmaceutical Product Approvals and Trends in 2012. BioProcess International https://bioprocessintl.com/manufacturing/monoclonal-antibodies/fda-biopharmaceutical-product-approvals-and-trends-in-2012-340619/ (2013).
2. Some, D. Biopharmaceutical Candidate Screening with Automated Dynamic Light Scattering. Chromatography Online https://www.chromatographyonline.com/view/biopharmaceutical-candidate-screening-automated-dynamic-light-scattering (2015).
3. Cockrell, G. M., Wolfe, M. S., Wolfe, J. L. & Schöneich, C. Photoinduced aggregation of a model antibody-drug conjugate. *Mol. Pharm.* **12**, 1784–1797 (2015).
4. Yu, Z., Reid, J. C. & Yang, Y.-P. Utilizing dynamic light scattering as a process analytical technology for protein folding and aggregation monitoring in vaccine manufacturing. *J. Pharm. Sci.* **102**, 4284–4290 (2013).
5. Menzen, T. & Friess, W. Temperature-ramped studies on the aggregation, unfolding, and interaction of a therapeutic monoclonal antibody. *J. Pharm. Sci.* **103**, 445–455 (2014).

Featured Products

DAWN® Multi-Angle static Light Scattering (MALS) detector by Wyatt Technology Corp.

Rating: ★★★★★

"DAWN HELEOS II is one of the best pieces of equipment for size, molecular mass and number density characterization. Along with SEC/FFF, this proves to be a highly advanced technology for comparability and analytical characterization of different biological molecules."

Dr. Vikas Bhat, BioMarin Pharmaceuticals

DynaPro Plate Reader Dynamic and Static Light Scattering Detector by Wyatt Technology Corp.

Rating: ★★★★★

"Great results interpretation, training and product support. Very easy setup, time saving, and great automation and HTS capability."

Dr. Yuchen Fan, Genentech

Calypso® Biomolecular Interaction Analysis System by Wyatt Technology Corp.

Rating: ★★★★★

"The Calypso II instrument, used in combination with a Wyatt Multi-Angle Light Scattering (MALS) instrument...allow for the collection of Composition-Gradient MALS data (CG-MALS)...The user is able to analyze the data by several different association models to determine how the molecules are interacting and how the size and population of the oligomers change with protein concentration and/or buffer conditions. The instrument is user-friendly, very robust and easy to maintain. The most valuable thing that I have gained from the instrument, aside from high quality results, is how much I have learned from the Wyatt application scientists regarding the fundamentals of protein interactions and how to interpret CG-MALS data...Wyatt Technology is a great company to work with!"

Dr. Katherine Bowers, FUJIFILM Diosynth Biotechnologies U.S.A., Inc.

Additional Resources

Poster

Aggregate analyses by light scattering – Complementary and orthogonal »

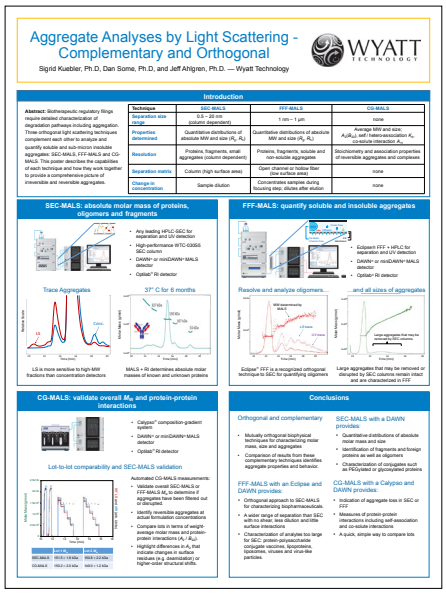

Webinars

Learn more about the benefits of light scattering techniques in this series of webinars from Wyatt Technology.

- **Predicting and evaluating the stability of therapeutic protein formulations by dynamic light scattering and machine learning »**
- **The importance of light scattering in biopharmaceutical formulation development »**
- **Biotherapeutics form and function: Case studies in light scattering »**
- **Rational use of dynamic light scattering for the characterization of cytokines, bispecific antibody fusion proteins and binary antibody mixtures »**
- **Predicting stability of antibody therapeutics by unfolded-state studies with high-throughput dynamic light scattering (HT-DLS) »**
- **Developing a toolkit towards prediction of protein aggregation »**
- **Advances in high-throughput screening of aggregation, stability and viscosity utilizing light scattering in microwell plates »**